

Predictive control barrier functions for piecewise affine systems with non-smooth constraints

Kanghui He, Anil Alan, Shengling Shi, *Member, IEEE*, Ton van den Boom, and Bart De Schutter, *Fellow, IEEE*

Abstract—Obtaining control barrier functions (CBFs) with large safe sets for complex nonlinear systems and constraints is a challenging task. Predictive CBFs address this issue by using an online finite-horizon optimal control problem that implicitly defines a large safe set. The optimal control problem, also known as the predictive safety filter (PSF), involves predicting the system’s flow under a given backup control policy. However, for non-smooth systems and constraints, some key elements, such as CBF gradients and the sensitivity of the flow, are not well-defined, making the current methods inadequate for ensuring safety. Additionally, for control-non-affine systems, the PSF is generally nonlinear and non-convex, posing challenges for real-time computation. This paper considers piecewise affine systems, which are usually control-non-affine, under nonlinear state and polyhedral input constraints. We solve the safety issue by incorporating set-valued generalized Clarke derivatives in the PSF design. We show that enforcing CBF constraints across all elements of the generalized Clarke derivatives suffices to guarantee safety. Moreover, to lighten the computational overhead, we propose an explicit approximation of the PSF. The resulting control methods are demonstrated through numerical examples.

Index Terms—Constrained control, piecewise affine systems, non-smooth control barrier functions, predictive control.

I. INTRODUCTION

A. Background

Motivated by emerging safety-critical applications such as autonomous driving [1] and automatic therapeutic regimens [2], control of nonlinear systems subject to state and input constraints has been receiving a growing attention in the academic community. Various safe control methods have been developed, such as model predictive control (MPC) [3], control barrier functions (CBFs)-based safety filters [4], solving Hamilton-Jacobi (HJ) reachability problems [5], and constrained reinforcement learning [6]. All methods have distinct advantages but also inherent limitations that hinder their practical effectiveness. In particular, MPC can be computationally expensive for hybrid and nonlinear systems; HJ reachability suffers from the curse of dimensionality; and constrained reinforcement learning [6].

This paper is part of a project that has received funding from the European Research Council (ERC) under the European Union’s Horizon 2020 research and innovation programme (Grant agreement No. 101018826 - CLariNet).

All authors are with Delft Center for Systems and Control, Delft University of Technology, Delft, The Netherlands (e-mail: k.he@tudelft.nl; a.alan@tudelft.nl; s.shi-3@tudelft.nl; a.j.j.vandenBoom@tudelft.nl; b.deschutter@tudelft.nl).

constrained reinforcement learning often lacks rigorous safety guarantees.

CBFs provide a modular framework with formal safety guarantees, called the CBF-based safety filter, to monitor and modify the potential unsafe control actions online. CBFs use their super-level sets to define control invariant sets, and the safety filter further involves a constrained optimization problem with CBF-based safety constraints to produce a safe control policy that keeps the system within the control invariant set. However, computing a permissive CBF, i.e., one associated with a non-conservative control invariant set, can be particularly challenging for nonlinear systems with both state and input constraints. As a result, CBF-based safety filters may be overly conservative.

Drawing inspiration from MPC, researchers have proposed to use model predictions to reduce the conservatism of CBFs both in discrete-time [7], [8] and in continuous-time domains [9], [10]–[12]. In particular, they use a finite-horizon constrained optimal control problem with a terminal CBF constraint to implicitly represent a larger control invariant set, resulting in a predictive safety filter (PSF). The terminal CBF is referred to as the backup CBF in [9]. For continuous-time control-affine systems, the PSF can be cast as convex quadratic programs, enabling efficient real-time implementation.

It should be emphasized that existing predictive CBF approaches for continuous-time systems are inherently limited to smooth systems and smooth safety constraints [9]–[12]. This requirement arises from the need to differentiate both the safety constraints and the system’s flow in the predictive CBF formulation. Furthermore, to allow for fast computation, these approaches concentrate on control-affine systems. For control-non-affine systems, the resulting safety filter usually involves solving a time-consuming non-convex nonlinear optimization problem.

Piecewise affine (PWA) systems can approximate general nonlinear systems to arbitrary precision and naturally capture hybrid behaviors [13]. On the other hand, PWA systems are generally control-non-affine and non-smooth. Therefore, the above-mentioned CBF-based safety filters cannot be directly adopted to efficiently provide safe control inputs for PWA systems.

B. Contributions

In this paper, we address the challenge of designing PSFs for continuous-time piecewise affine (PWA) systems subject

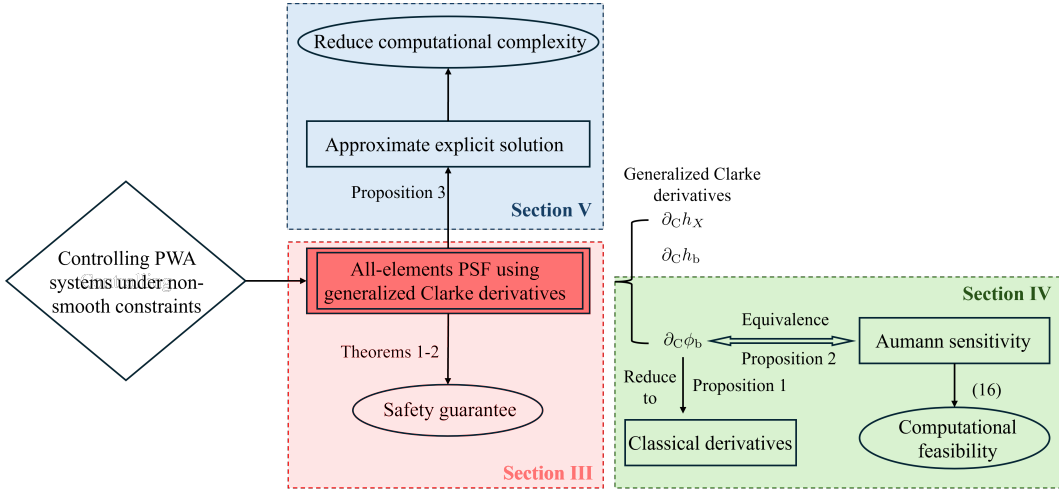


Fig. 1: Graphical representation of the paper structure.

to arbitrary, possibly non-smooth, Lipschitz continuous state constraints¹ and polyhedral input constraints. The resulting PSF is formulated as a mixed-integer quadratic programming (MIQP) problem. The main contributions of this paper, in comparison to the state of the art, are:

1. We propose a novel PSF that uses generalized Clarke derivatives to enforce safety constraints. This framework is applicable to any Lipschitz continuous but non-smooth CBF and any continuous PWA system with Lipschitz continuous but non-smooth state constraints. We rigorously analyze the safety guarantees of the resulting control policy (Lemma 2 and Theorem 2).

2. We present a tractable approach for computing the generalized Clarke derivative (Clarke sensitivity) of the system's flow. In particular, we introduce an alternative Aumann sensitivity and show their equivalence. Notably, the Aumann sensitivity can be efficiently computed through numerical integration of the system.

3. To reduce the computational complexity of solving the MIQP corresponding to the PSF online, we introduce an explicit approximation of the PSF. This approximation is provably feasible and significantly lowers the online computational burden.

4. Additionally, the theoretical safety result (Lemma 2) generalizes classical CBF conditions that require continuous differentiability to encompass CBFs that are merely Lipschitz continuous. This extension applies to general nonlinear systems, not just PWA ones.

The paper's main results and their organization are shown in Fig. 1.

C. Related work

(Approximate) MPC for PWA systems. Hybrid MPC is widely used to control PWA systems under linear state and input constraints [3]. In the hybrid MPC formulation, the

PWA system is equivalently transformed into a mixed-logical dynamical (MLD) system that includes both continuous and discrete state and input variables [13]. This transformation allows the MPC problem to be formulated as a mixed-integer convex quadratic or linear optimization problem, which is solved online to generate safe control inputs. Explicit MPC is an offline version of hybrid MPC, which offline computes and stores the map from the state to the solution of the MPC problem by multi-parametric programming [14]. However, MPC methods struggle with significant computational challenges in high-dimensional systems, either due to solving complex mixed-integer problems or evaluating intricate explicit control laws.

This limitation of MPC motivates the research of approximating MPC control laws, by using, e.g., PWA simplicial functions [15], neural networks [6], sampling-based polytopic trees [16], and minimum-time objective functions [17]. Another promising approach to simplify the MPC problem is to employ reinforcement learning [18] or supervised learning [19], [20] to determine the values of the discrete decision variables, effectively reducing the mixed-integer problem to a convex optimization problem. However, while exact MPC offers formal performance guarantees, it leads to a high computational burden, especially for nonlinear, non-convex constraints. Approximate MPC, on the other hand, still has open challenges regarding stability, robustness, and sample complexity.

Predictive safety filters. Research in both the continuous-time and discrete-time domains has contributed to the development of PSFs, which aim to reduce the conservatism of standard safety filters. Representative work includes [7], [8] in the discrete-time domain and [9]–[12] (sometimes also called backup CBFs) in the continuous-time domain. Based on [7], the authors in [21]–[23] approximate discrete-time predictive CBFs using neural networks to reduce the computational burden of safety filters. The work in [24] extends the PSFs of [9], [11] to guaranteeing safe behavior for complex systems by designing safety filters for reduced-order models. However, continuous-time predictive CBF methods are fundamentally

¹We say that a constraint $x \in X$ is continuous if X can be represented by the level set of a continuous function, i.e., $X = \{x|f(x) \leq 0\}$, where f is continuous.

limited to smooth systems and smooth safety constraints. As mentioned before, this requirement arises from the need to differentiate both the safety constraints and the system's flow in the predictive CBF formulation, which requires computing the Jacobian of the closed-loop dynamics with a smooth backup controller. Moreover, to date, there is no related work addressing the design of PSFs for PWA systems.

Non-smooth CBFs. [25] proposes non-smooth CBFs for deterministic multi-agent systems, leveraging generalized gradients to ensure forward invariance. This result has been employed in applications where non-smooth safety constraints naturally arise, such as obstacle avoidance involving ellipsoids and polytopes [26] and network connectivity maintenance [27]. Besides, formulating multiple constraints with “min” and “max” functions will generally result in a non-smooth CBF. Building on [25], [26] extends non-smooth CBFs to stochastic systems. Related to these techniques, piecewise continuous CBFs are introduced in [28], where the authors of [28] argue that, in addition to satisfying the CBF inequality, a tangent cone condition at the boundary of the safe set should also be enforced to ensure forward invariance. Meanwhile, Cohen *et al.* [29] take a different perspective by smoothing the solution to CBF-based safety filters using the Implicit Function Theorem, rather than focusing on the smoothness of the CBFs themselves. All of the above approaches focus on classical CBFs with no predictions. This means that the analysis primarily addresses the non-smoothness of the CBF itself. In contrast, the non-smoothness in our setting arises not only from the structure of the CBF but also from state constraints and the PWA dynamics, making it more challenging to derive safety guarantees.

D. Notations

The set of real vectors with the dimension n is denoted by \mathbb{R}^n . The sets \mathbb{N} and \mathbb{N}^+ represent the set of non-negative integers and the set of positive integers, respectively. Furthermore, $\mathbb{N}_a = \{0, 1, \dots, a\}$ and $\mathbb{N}_a^+ = \{1, 2, \dots, a\}$. The norm $\|x\|$ is the Euclidean norm of the vector x , and $\|A\|$ is the induced norm of the Euclidean norm for the matrix A . The notation $\text{int}(S)$ refers to the interior of the set S , and $\text{clo}(S)$ is the closure of the set S . Besides, 1_n is the vector of ones with n elements, and I_n is the identity matrix with dimension $n \times n$. A continuous function $\alpha : [0, \infty) \rightarrow [0, \infty]$ is said to belong to class \mathcal{K}_∞ if it is strictly increasing and if $\alpha(0) = 0$ and $\lim_{r \rightarrow \infty} \alpha(r) = \infty$. The step function $\text{step}(\cdot)$ returns 1 if the input is non-negative, and 0 otherwise. The notation $Df(x_0) \in \mathbb{R}^{m \times n}$ represents the derivative of the differentiable function $f(\cdot) : \mathbb{R}^n \rightarrow \mathbb{R}^m$ at x_0 .

II. PRELIMINARIES AND BACKUP CBFs

Consider a general continuous-time nonlinear system of the form

$$\dot{x} = f(x, u), \quad (1)$$

where $x \in \mathbb{R}^n$ is the state, $u \in \mathbb{R}^m$ is the input, and $f(\cdot) : \mathbb{R}^{n+m} \rightarrow \mathbb{R}^n$ is globally Lipschitz continuous. The system must always satisfy the given state constraint $x \in X :=$

$\{x \in \mathbb{R}^n | h_X(x) \geq 0\}$ and input constraint $u \in U$. Here, the function $h_X(\cdot) : \mathbb{R}^n \rightarrow \mathbb{R}$ is locally Lipschitz continuous, and U is a polyhedron².

A. Control barrier functions

CBFs offer an effective approach for designing safe control systems.

Definition 1 (Control barrier function [30]). A continuously differentiable function $h(\cdot) : \mathbb{R}^n \rightarrow \mathbb{R}$ is a *control barrier function* for (1) if there exists an $\alpha \in \mathcal{K}_\infty$ such that

$$\sup_{u \in U} \dot{h}(x, u) = \sup_{u \in U} \{\nabla h(x) \cdot f(x, u)\} \geq -\alpha(h(x)) \quad (2)$$

holds for any $x \in S := \{x \in \mathbb{R}^n | h(x) \geq 0\}$.

With a CBF available, there always exists a controller $\pi(\cdot) : \mathbb{R}^n \rightarrow \mathbb{R}^m$ satisfying $\pi(x) \in U$ and $\nabla h(x) \cdot f(x, \pi(x)) \geq -\alpha(h(x))$ for all $x \in S$. This controller will render S forward invariant for (1), and S is called the safe set [30]. Under the supplemental condition $S \subseteq X$, the controller π makes the system always satisfy the constraints if the initial state is within S .

B. Predictive safety filters for smooth systems

For nonlinear systems, it is nontrivial to get a permissive CBF, i.e., a CBF with a large safe set S [31]. Drawing ideas from model predictive control, PSFs address this issue using model predictions [10], [24]. We recall this method in this subsection.

First, a CBF $h_b : \mathbb{R}^n \rightarrow \mathbb{R}$ and an associated safe controller π_b , satisfying (i) $\pi_b(x) \in U$ for all $x \in X$, and (ii) $\nabla h_b(x) \cdot f(x, \pi_b(x)) \geq -\alpha_b(h_b(x))$ for all $x \in S_b := \{x \in \mathbb{R}^n | h_b(x) \geq 0\} \subseteq X$, are obtained based on existing methods such as LQR or sum-of-squares programming [32], depending on the form of the system. Here, the subscript “b” refers to “backup”.

The closed-loop system with the backup controller can be written as

$$\dot{x} = f_b(x) := f(x, \pi_b(x)) \quad (3)$$

If f and π_b are globally Lipschitz continuous, which is commonly the case in many practical scenarios, including linear, PWA, and polynomial systems and policies, then for any $x(0) = x_0 \in \mathbb{R}^n$, according to [33, Theorem 3.2], the system (3) has a unique solution $x(t) = \phi_b(x_0, t)$, $\forall t \in [0, \infty)$.

Definition 2 (Constrained reachable set). Given the system (3) and the set X , for any set S and any time $T > 0$, the T -step constrained reachable set for (3) is defined as $\Phi_{\text{const}}(S, T) := \{x \in \mathbb{R}^n | \phi_b(x, \tau) \in X, \forall \tau \in [0, T] \wedge \phi_b(x, T) \in S\}$.

The PSF method uses an important property related to constrained reachable sets, stating that the constrained reachable sets of any invariant set S are always controlled-invariant and are supersets of S . See [24, Lemma 1] and [9, Proposition 2]

²While the results of this paper can be extended to cases where U is a union of polyhedra, we assume for simplicity that U is a single polyhedron

for a more precise statement. This invariance property allows us to synthesize a safe controller that has a larger safe region.

Lemma 1 (Safety of backup CBFs [9], [24]). Consider the system (1) with the state and input constraints $x \in X$ and $u \in U$, the backup controller π_b , and the backup CBF h_b . Suppose that f , h_X , and h_b and π_b are continuously differentiable and that X is compact. Then, there exist a controller $\pi_{\text{safe}}(\cdot) : \mathbb{R}^n \rightarrow \mathbb{R}^m$ and $\alpha, \alpha_b \in \mathcal{K}_\infty$ such that the following conditions hold $\forall T \geq 0$ and $\forall x \in \Phi_{\text{const}}(S_b, T)$:

$$\begin{aligned} \dot{h}_X(\phi_b(x, \tau), \pi_{\text{safe}}(x)) &\geq -\alpha(h_X(\phi_b(x, \tau))), \forall \tau \in [0, T] \\ \dot{h}_b(\phi_b(x, T), \pi_{\text{safe}}(x)) &\geq -\alpha_b(h_b(\phi_b(x, T))) \\ \pi_{\text{safe}}(\phi_b(x, \tau)) &\in U, \forall \tau \in [0, T]. \end{aligned} \quad (4)$$

Moreover, any locally Lipschitz continuous controller π_{safe} that satisfies (4) renders $\Phi_{\text{const}}(S_b, T)$ forward invariant for (1).

The proof of Lemma 1 relies on verifying that

$$h(x) := \min \left\{ \min_{\tau \in [0, T]} h_X(\phi_b(x, \tau)), h_b(\phi_b(x, T)) \right\}, \quad (5)$$

is a valid CBF. We call the function h in (5) the *predictive CBF*.

Lemma 1 can be directly employed for safe controller synthesis by designing the following optimization-based PSF³:

$$\begin{aligned} &\pi_{\text{safe}}(x) \\ &= \underset{u \in U}{\text{argmin}} \|u - \pi_r(x)\|^2 \\ &\text{s.t. } \dot{h}_X(\phi_b(x, \tau), u) \geq -\alpha(h_X(\phi_b(x, \tau))), \forall \tau \in [0, T] \\ &\quad \dot{h}_b(\phi_b(x, T), u) \geq -\alpha_b(h_b(\phi_b(x, T))), \end{aligned} \quad (6)$$

where $T \geq 0$ is the prediction horizon and $\pi_r(\cdot) : \mathbb{R}^n \rightarrow \mathbb{R}^m$ is a reference controller. Problem (6) is, in general, nonlinear and non-convex. In existing literature, a control-affine system and a polyhedral U are usually considered, which makes (6) a convex quadratic program (QP) (after discretizing $[0, T]$) [10], [11], [24]. Besides, thanks to the existence of π_b , problem (6) is guaranteed to be feasible $\forall x \in \Phi_{\text{const}}(S_b, T)$.

For the continuously differentiable system (1), the derivatives \dot{h}_X and \dot{h}_b in (6) can be expressed as

$$\dot{h}_X(\phi_b(x, \tau), u) = Dh_X(\phi_b(x, \tau)) \frac{\partial \phi_b(x, \tau)}{\partial x} f(x, u) \quad (7)$$

$$\dot{h}_b(\phi_b(x, T), u) = Dh_b(\phi_b(x, T)) \frac{\partial \phi_b(x, T)}{\partial x} f(x, u), \quad (8)$$

where $\frac{\partial \phi_b(x, \tau)}{\partial x} \in \mathbb{R}^{n \times n}$ is called the sensitivity of the flow to its initial condition⁴.

Remark 1. Note that the backup controller π_b is a virtual controller that is never applied. It is only used to derive the CBF constraints in (6). The applied controller is π_{safe} .

³The conditions under which π_{safe} is locally Lipschitz, which is required in Lemma 1, can be found in [34].

⁴In (6), x refers to the initial condition of the safety filter, which is also the current state of the system (1).

C. Problem statement

In this paper, we focus on a class of continuous PWA systems:

$$\dot{x} = f_{\text{PWA}}(x, u) := A_i x + B_i u + c_i, \text{ for } \begin{bmatrix} x \\ u \end{bmatrix} \in \mathcal{P}_i, \quad (9)$$

where $f_{\text{PWA}} : \mathbb{R}^{n+m} \rightarrow \mathbb{R}^n$ is a continuous PWA function, $\{\mathcal{P}_i\}_{i=1}^p$ constitutes a strict polyhedral partition [3, Definition 4.5] of the state-input space. The union of all boundaries of all \mathcal{P}_i , $i \in \mathbb{N}_p^+$ is called the boundary of the PWA system.

Computing the time derivatives in (7) is an essential step for designing the safety filter (6). It should be noted that existing literature usually assumes that the system, the CBF, and the constraint X are continuously differentiable [10], [11], [24]. In this case, the terms on the right-hand side of (7) are well-defined and safety performance is guaranteed (Lemma 1). However, the PWA system is usually not continuously differentiable at the boundary of each \mathcal{P}_i , and many widely existing constraints, such as polytopic constraints, are not differentiable everywhere. This means that the time derivatives in (7) may have multiple possible values and that the results in Lemma 1 may not hold.

Secondly, for control-affine systems, problem (6) can be formulated as a convex QP, which is computationally inexpensive to solve in real time. However, as observed in (9), $f_{\text{PWA}}(x, u)$ does not depend linearly on u . In this case, problem (6) becomes an MIQP, which needs much more computational effort to solve than a convex QP.

In the remainder, the following problems will be addressed.

Problem 1 (addressed in Section III): How to design a PSF with safety guarantees for a given PWA system, which should address the non-smoothness of the PWA dynamics, the state constraint, and the CBF h_b ?

Problem 2 (addressed in Section IV): How to overcome the computational intractability of the critical component of the safety filter, in particular, the not well-defined sensitivity for PWA systems?

Problem 3 (addressed in Section V): How to approximate the solution to the safety filter in a computationally efficient way to enable swift online implementation?

D. Generalized sensitivity

For non-smooth functions, the concept of the Jacobian matrix from smooth functions can be generalized using several approaches, such as the generalized Clarke derivative [35] and Mordukhovich subdifferential [36]. In this paper, we advocate for the use of the generalized Clarke derivative due to its convenience in performance analysis. The generalized Clarke derivative extends the idea of the Jacobian matrix to Lipschitz continuous functions that may not be differentiable everywhere.

Definition 3 (Generalized Clarke derivative [35]). The *generalized Clarke derivative* of a locally Lipschitz continuous function $\phi(\cdot) : \mathbb{R}^n \rightarrow \mathbb{R}^{n_\phi}$, denoted by $\partial_C \phi$, is defined as

$$\begin{aligned} \partial_C \phi(x) &= \\ &\text{conv} \left\{ \lim_{i \rightarrow \infty} D\phi(x_i) \mid x_i \rightarrow x, \phi \text{ is differentiable at } x_i \right\}, \end{aligned}$$

where $D\phi(x_i) \in \mathbb{R}^{n_\phi \times n}$ is the classical Jacobian at points x_i where ϕ is differentiable. The notation n_ϕ refers to the image dimension of ϕ .

Note that for a locally Lipschitz function, the generalized Clarke derivative is nonempty, compact, convex, and set-valued [35]. It is the convex hull of the limits of classical Jacobian sequences at nearby points where the function is differentiable. If a function is differentiable at a point, the generalized Clarke derivative reduces to the classical Jacobian at that point.

III. SAFE CONTROLLER SYNTHESIS

For PWA systems, piecewise linear feedback controllers are often designed in the literature [37]. The PWA system (9) controlled by a piecewise linear backup controller can therefore be written as

$$\dot{x} = f_{\text{PWA},b}(x) := D_i x + d_i, \text{ for } x \in \mathcal{R}_i. \quad (10)$$

In (10), $f_{\text{PWA},b} : \mathbb{R}^n \rightarrow \mathbb{R}^n$ is a globally continuous PWA function, and $\{\mathcal{R}_i\}_{i=1}^r$ constitutes a strict polyhedral partition of the state space. Since (10) has a global Lipschitz constant $L = \max_{i \in \mathbb{N}_r^+} \|D_i\|$, we can denote the unique solution with any initial condition $x(0) = x_0 \in \mathbb{R}^n$ by $x(\tau) = \phi_b(x_0, \tau)$, $\forall \tau \in [0, \infty)$. Furthermore, according to [33, Theorem 3.4], for any two initial states x_0 and y_0 , the solutions of (10) satisfy $\|\phi_b(x_0, \tau) - \phi_b(y_0, \tau)\| \leq \|x_0 - y_0\| \exp(L\tau)$, $\forall \tau > 0$. This proves the Lipschitz continuous dependence of $\phi_b(x_0, \tau)$ on the initial state x_0 in \mathbb{R}^n for any finite τ .

Considering the case when ϕ_b , h_b , and h_X is not necessarily differentiable, and based on the design of PSFs for smooth systems in (6), we design the following PSF utilizing the generalized Clarke derivatives of ϕ_b , h_b , and h_X :

All-elements PSF:

$$\begin{aligned} & \pi_{\text{safe}}(x) \\ &= \underset{u \in U}{\text{argmin}} \|u - \pi_r(x)\|^2 \end{aligned} \quad (11a)$$

$$\begin{aligned} & \text{s.t. } \partial h_X Q f_{\text{PWA}}(x, u) \geq -\alpha(h_X(\phi_b(x, \tau))), \\ & \quad \forall \partial h_X \in \partial_C h_X(\phi_b(x, \tau)), \forall Q \in \partial_C \phi_b(x, \tau), \forall \tau \in [0, T] \end{aligned} \quad (11b)$$

$$\begin{aligned} & \partial h_b Q f_{\text{PWA}}(x, u) \geq -\alpha_b(h_b(\phi_b(x, T))), \\ & \quad \forall \partial h_b \in \partial_C h_b(\phi_b(x, T)), \forall Q \in \partial_C \phi_b(x, T), \end{aligned} \quad (11c)$$

where $\partial_C \phi_b(x, \tau)$ is called the *Clarke sensitivity*. Different from (6) in which the CBF constraints are uniquely determined by the unique sensitivity matrix $\frac{\partial \phi_b}{\partial x}$ and the unique derivatives Dh_X and Dh_b , we require that the CBF constraints should be satisfied for *all* elements contained in the sets $\partial_C h_X$, $\partial_C h_b$, and $\partial_C \phi_b$.

A. Performance analysis

Before deriving a computationally tractable way to compute the Clarke sensitivity and to solve (11), we first analyze the safety performance of π_{safe} .

Assumption 1. (i) $\pi_b(x) \in U$, for all $x \in X$;

(ii) $\partial h_b f_{\text{PWA},b}(x) \geq -\alpha_b(h_b(x))$, for all $x \in S_b := \{x \in \mathbb{R}^n | h_b(x) \geq 0\} \subseteq X$ and for all $\partial h_b \in \partial_C h_b(x)$.

Assumption 1 is reasonable and aligns with similar assumptions commonly found in the literature on predictive CBFs [10], [24] and MPC frameworks that incorporate CBFs or control Lyapunov functions for designing terminal constraints [9]. The key distinction in our assumption is that it requires the CBF constraint to hold for all elements in the Clarke generalized gradient of h_b , rather than relying solely on the unique classical gradient as typically assumed in existing works. If h_b is smooth, then Assumption 1 becomes equivalent to other assumptions in literature, such as [24, Assumption 1].

Theorem 1 (Feasibility). Consider the continuous PWA system (9), the piecewise linear backup controller π_b , the Lipschitz continuous h_X and h_b , and the proposed PSF (11). Suppose that Assumption 1 holds and that X is compact. Then, there exist $\alpha, \alpha_b \in \mathcal{K}_\infty$ such that problem (11) is feasible for any $x \in \Phi_{\text{const}}(S_b, T)$ and any $T \geq 0$.

Proof. We will prove that the backup solution $\pi_b(x)$ is a feasible solution to (11). To do so, for any $\tau \in [0, T]$, we need to consider several cases depending on the differentiability of the functions ϕ_b , h_b , and h_X . For clarity and without loss of generality, we consider the following two cases: (i) $\phi_b(x, \tau)$ is differentiable, and (ii) $\phi_b(x, \tau)$ is not differentiable. The same reasoning applies analogously when considering the differentiability or non-differentiability of h_b and h_X , and thus we omit the cases for these two functions for brevity.

(i) If $\phi_b(x, \tau)$ is differentiable w.r.t. x at $x = \bar{x}$, then $\partial_C \phi_b(x, \tau)$ reduces to the classical sensitivity $\frac{\partial \phi_b(x, \tau)}{\partial x}$ and therefore the feasibility of $\pi_b(x)$ follows from Lemma 1.

(ii) If $\phi_b(x, \tau)$ is not differentiable w.r.t. x at $x = \bar{x}$, noting Definition 3, consider any sequence $\{x_i\}_{i=0}^\infty$ converging to \bar{x} and satisfying that $\phi_b(x, \tau)$ is differentiable w.r.t. x at x_i . It follows from the analysis in the first case that by letting $u_i = \pi_b(x_i)$, we have that

$$Dh_X(\phi_b(x_i, \tau)) \frac{\partial \phi_b(x_i, \tau)}{\partial x_i} f_{\text{PWA}}(x_i, u_i) \geq -\alpha(h_X(\phi_b(x_i, \tau)))$$

holds. By taking the limit $i \rightarrow \infty$ and noting that $\lim_{i \rightarrow \infty} \frac{\partial \phi_b(x_i, \tau)}{\partial x_i} \in \partial_C \phi_b(\bar{x}, \tau)$ by Definition 3, we get the feasibility of (11b). An analogous argument can be applied to prove the feasibility of (11c). The proof of Theorem 1 is completed. \square

To establish the forward invariance of $\Phi_{\text{const}}(S_b, T)$, i.e., the infinite-horizon safety of π_{safe} , we introduce the following key lemma based on the comparison theorem [33, Lemma 3.4]. This lemma is applicable to invariance analysis for general nonlinear systems involving any non-smooth CBF.

Lemma 2. Consider the system (1). Suppose that there exist a Lipschitz continuous controller $\pi(\cdot) : \mathbb{R}^n \rightarrow \mathbb{R}^m$, a Lipschitz continuous $h(\cdot) : \mathbb{R}^n \rightarrow \mathbb{R}$, and a Lipschitz continuous function $\alpha \in \mathcal{K}_\infty$ such that

$$\begin{aligned} & \partial h(x) f(x, \pi(x)) \geq -\alpha(h(x)), \\ & \forall x \in \{x \in \mathbb{R}^n | h(x) \geq 0\} \text{ and } \forall \partial h(x) \in \partial_C h(x). \end{aligned} \quad (12)$$

As a result, if $h(x_0) \geq 0$, we have $h(\phi(x_0, t)) \geq 0$, $\forall t \geq 0$, where $\phi(x_0, t)$ is the solution of the system (1) controlled by π , starting from x_0 .

Proof. See Appendix A. \square

Remark 2. The result in Lemma 2 establishes the forward invariance of $\{x \in \mathbb{R}^n | h(x) \geq 0\}$. This result extends safety guarantees from continuously differentiable CBFs to CBFs that are merely Lipschitz continuous. More importantly, in contrast to the non-smooth CBF analysis in [25], we do not require $\dot{h}(t) \geq -\alpha(h(t))$ for almost every t .

With the safety guarantees of non-smooth CBFs given in Lemma 2, we are ready to present the main result on the safety of π_{safe} .

Theorem 2 (Forward invariance). Consider the continuous PWA system (9), the piecewise linear backup controller π_b , the Lipschitz continuous backup CBF h_b , and the proposed all-elements PSF (11). If Assumption 1 holds and the policy π_{safe} is locally Lipschitz continuous, then π_{safe} renders $\Phi_{\text{const}}(S_b, T)$ forward invariant.

Proof. Given $T \geq 0$, like [10], we consider the CBF candidate in (5), which is Lipschitz continuous and satisfies $\Phi_{\text{const}}(S_b, T) = \{x \in \mathbb{R}^n | h(x) \geq 0\}$ according to [10, Lemma 2].

For each $x \in \Phi_{\text{const}}(S_b, T)$, based on (5), we can distinguish two cases: (i) $h(x) = h_X(\phi_b(x(t), \tau'))$ with a certain $\tau' \in [0, T]$ and (ii) $h(x) = h_b(\phi_b(x(t), T))$.

For the first case, we define the composite function $h_\phi = h_X \circ \phi_b$. Given $\tau' \in [0, T]$, we have the following expression for the Clarke derivative of the composite function [38, Theorem 2.3.9]:

$$\begin{aligned} & \partial_C h_\phi(x, \tau') \\ & \subseteq \text{conv} \{ \partial h_X Q, \partial h_X \in \partial_C h_X(\phi_b(x, \tau')), Q \in \partial_C \phi_b(x, \tau') \}. \end{aligned}$$

Then, we can apply the chain rule to obtain the Clarke derivative of the composite function h , that is, for any $\partial h \in \partial_C h(x)$,

$$\begin{aligned} & \partial h f_{\text{PWA}}(x, \pi_{\text{safe}}(x)) + \alpha(h(x)) \\ & = \partial h_\phi f_{\text{PWA}}(x, \pi_{\text{safe}}(x)) + \alpha(h_X(x)), \exists \partial h_\phi \in \partial_C h_\phi(x, \tau') \\ & = \partial h_X Q f_{\text{PWA}}(x, \pi_{\text{safe}}(x)) + \alpha(h_X(\phi_b(x, \tau'))), \\ & \exists \partial h_X \in \partial_C h_X(\phi_b(x, \tau')), Q \in \partial_C \phi_b(x, \tau') \\ & \geq 0, \end{aligned} \quad (13)$$

where the second equality is obtained by applying the chain rule to $\partial_C h_\phi$, and the last line follows from the fact that π_{safe} satisfies the constraint (11b).

An analogous argument to that in (13) can be applied for the second case, yielding $\partial h f_{\text{PWA}}(x, \pi_{\text{safe}}(x)) + \alpha_b(h(x)) \geq 0$ for any $\partial h \in \partial_C h(x)$.

As a consequence, the CBF candidate h satisfies (12) in Lemma 2. If π_{safe} is locally Lipschitz continuous, applying Lemma 2 yields $h(\phi_{\text{safe}}(x_0, t)) \geq 0$, $\forall t \geq 0$, if $x_0 \in \Phi_{\text{const}}(S_b, T)$. Here, $\phi_{\text{safe}}(x_0, t)$ is the solution of the system (9) starting from x_0 controlled by π_{safe} . This proves the forward invariance of $\Phi_{\text{const}}(S_b, T)$ under π_{safe} . \square

Theorems 1 and 2 state that when there are non-smooth CBF constraints, the all-elements PSF can ensure that the system always satisfies the constraints, provided that π_{safe} is locally Lipschitz continuous. Analyzing the conditions under which π_{safe} is Lipschitz continuous is left for future work.

IV. NON-SMOOTH ANALYSIS OF PWA SYSTEMS

In the previous section, we have shown sufficient conditions to ensure formal guarantees for feasibility and safety for the proposed all-element PSF (11). However, To construct the proposed PSF, we need to compute the generalized Clarke derivative for ϕ_b (Clarke sensitivity) and the generalized Clarke derivatives $\partial_C h_X$ and $\partial_C h_b$. Computing $\partial_C h_X$ and $\partial_C h_b$ is generally feasible, since their explicit forms are usually known. Finding a generalized Clarke derivative for ϕ_b requires computing classical Jacobians for all converging sequences x_i where ϕ_b is differentiable, and it is generally intractable. This section addresses this challenge for the considered PWA system.

The following definition is useful for characterizing the behavior of PWA systems:

Definition 4 (Time-stamped switching sequence). Consider the PWA system (10). Given the initial state x_0 , the *time-stamped switching sequence* of the solution $\phi_b(x_0, \tau)$, denoted as

$$\Gamma(x_0) = \{(\tau_0, I_0), (\tau_1, I_1), \dots, (\tau_M, I_M)\}, \quad \text{with } I_k \subseteq \mathbb{N}_r^+, \forall k \in \mathbb{N}_M, \quad (14)$$

is the ordered sequence of time instants and the indices of regions such that

- $\tau_0 = 0$ and $x_0 \in \text{clo}(\mathcal{R}_{I_0})$;
- $\phi_b(x_0, \tau) \in \text{clo}(\mathcal{R}_i)$, $\forall i \in I_k$ and $\forall \tau \in [\tau_k, \tau_{k+1})$;
- $I_k \neq I_{k+1}$, $\forall k \in \mathbb{N}_{M-1}$ and $\tau_0 < \tau_1 < \dots < \tau_M$.

In (14), r is the number of polyhedral regions of (10) and M is the number of switching times.

The switching sequence can be infinite, i.e., $M = \infty$, meaning that the system exhibits zeno behavior if τ_M is finite or chattering if $\tau_M = \infty$. Besides, each I_k can contain more than one element. In this case, the system operates on the shared boundary of multiple regions of (10) during $[\tau_k, \tau_{k+1})$. If I_k consists of multiple elements, then we define $\mathcal{R}_{I_k} := \bigcup_{i \in I_k} \mathcal{R}_i$.

A. Aumann sensitivity for PWA systems

In this subsection, we propose an alternative and computable generalized sensitivity $Q_A(x_0, \tau)$ using the Aumann integral [39]. In subsequent subsections, we will show that, under certain assumptions, this formulation is equivalent to the Clarke sensitivity.

Definition 5 (Aumann sensitivity). Consider the PWA system (10) and its solution ϕ_b . The *Aumann sensitivity* for any initial state x_0 at time τ , denoted by $Q_A(x_0, \tau)$, is implicitly defined

by

$$\begin{aligned} Q_A(x_0, \tau) := & \{Q(x_0, \tau) \mid Q(x_0, \tau) = I_n \\ & + \int_0^\tau \partial f_{\text{PWA}, b}(\phi_b(x_0, s)) Q(x_0, s) ds, \\ & \partial f_{\text{PWA}, b}(x) \in \{D_i \mid i \text{ s.t. } x \in \text{clo}(\mathcal{R}_i)\}\}. \end{aligned} \quad (15)$$

The Aumann integral is introduced to handle cases where the integration is carried out on all possible values of the integrand. As a result, the Aumann sensitivity naturally becomes a set-valued function. When this sensitivity takes a single value at a point, it coincides with the classical Jacobian of ϕ_b at that point.

Given the initial state x_0 , denote by $I(x_0)$ the Cartesian product of the switching sequence $\{I_0, I_1, \dots, I_M\}$. With this definition, the Aumann sensitivity is expressed as:

$$\begin{aligned} & Q_A(x_0, \tau) \\ &= \left\{ Q(x_0, \tau) \mid \begin{array}{l} Q(x_0, \tau) = I + \sum_{k=0}^{\bar{k}} \int_{\tau_k}^{\min\{\tau, \tau_{k+1}\}} D_{i_k} Q(x_0, s) ds, \\ (i_0, i_1, \dots, i_M) \in I(x_0) \end{array} \right\}, \tau \in [\tau_{\bar{k}}, \tau_{\bar{k}+1}), \bar{k} \leq M-1. \end{aligned} \quad (16)$$

Each Q is single-valued and can be obtained by the standard sensitivity computation [33, Chapter 3.3]. The cardinality of $Q_A(x_0, \tau)$ is less than or equal to $\prod_{k \in \mathbb{N}_M} |I_k|$.

B. Properties of the Aumann sensitivity

The ultimate objective of this section is to show the equivalence between the Aumann sensitivity and the Clarke sensitivity. Before doing that, we first study the properties of the Aumann sensitivity.

Without loss of generality, suppose that the closure of each \mathcal{R}_i admits the hyperplane representation $\{x \in \mathbb{R}^n \mid H_i x + h_i \leq 0\}$, where $H_i \in \mathbb{R}^{m_i \times n}$, $h_i \in \mathbb{R}^{m_i}$, and m_i is the number of inequalities that constitute \mathcal{R}_i . Denote by

$$\Gamma_I := \{x \in \mathbb{R}^n \mid \bar{g}_I(x) := g_I x + b_I = 0\}$$

the common boundary of two or more adjacent regions \mathcal{R}_I , where I is a set of indices of the adjacent regions. Here, $g_I \in \mathbb{R}^{n_{g_I} \times n}$, $b_I \in \mathbb{R}^{n_{g_I}}$, and $\bar{g}_I(\cdot) : \mathbb{R}^n \rightarrow \mathbb{R}^{n_{g_I}}$.

From (15) we know that Q_A could take multiple values if the solution ϕ_b stays on the common boundary of some regions of (10) during a period. This is because during that period, the integral term can take multiple values. This motivates us to check if there is a non-empty set on the boundary such that the solution ϕ_b belongs to this set during a certain period. We consider the following *critical set* (could be empty):

$$\begin{aligned} \mathcal{C} &:= \bigcup_{I \in \mathcal{I}} \mathcal{C}_I, \text{ where } \mathcal{C}_I = \bigcap_{i \in I} \text{clo}(\mathcal{R}_i) \\ \mathcal{I} &:= \{I \subseteq \mathbb{N}_r^+ \mid \{\mathcal{R}_i\}_{i \in I} \text{ are adjacent, } \bar{g}_I^{(q)} = 0, \forall q \in \mathbb{N}_n, \\ & \text{and } \exists i, j \in I \text{ s.t. } D_i \neq D_j\}. \end{aligned} \quad (17)$$

In (17), $\bar{g}_I^{(q)}$ is the q -th order element-wise time derivative of \bar{g}_I along the PWA system (10). Because the first q order time derivatives of \bar{g}_I are zero, \bar{g}_I remains constant according to the Cayley–Hamilton Theorem [40]. Therefore, we can interpret \mathcal{C} as the set where the trajectory is possible to stay on a boundary $\bar{g}_I(x) = 0$ of some polyhedra \mathcal{R}_i , $i \in I$ for some periods.

For any initial state x_0 , define the *forward reachable set* as $\Phi_{\text{for}}(x_0) := \bigcup_{\tau \in [0, \infty)} \{\phi_b(x_0, \tau)\}$. Similarly, for any set S of states, define the *backward reachable set* $\Phi_{\text{back}}(S) := \{x \in \mathbb{R}^n \mid \exists \tau \in [0, \infty) \text{ s.t. } \phi_b(x, \tau) \in S\}$. We have the following result on the relation among \mathcal{C} , Q_A , and the classical Jacobian (if it exists).

Proposition 1. The following statements are equivalent:

- (1) The classical Jacobian $\frac{\partial \phi_b(x_0, \tau)}{\partial x_0}$ of $\phi_b(x_0, \tau)$ exists at $x_0 = \bar{x}_0$ for all $\tau \geq 0$.
- (2) The Aumann sensitivity $Q_A(x_0, \tau)$ is single-valued at $x_0 = \bar{x}_0$ for all $\tau \geq 0$.
- (3) $\Phi_{\text{for}}(\bar{x}_0) \cap \mathcal{C} = \emptyset$.
- (4) $\bar{x}_0 \notin \Phi_{\text{back}}(\mathcal{C})$.

As a consequence, if \mathcal{C} is empty, the Aumann sensitivity Q_A defined in (15) is single-valued for any x_0 , which implies the global existence of the classical Jacobian $\frac{\partial \phi_b(x_0, \tau)}{\partial x_0}$.

Proof. See Appendix B. \square

The critical set \mathcal{C} is a union of some polyhedra \mathcal{C}_I , $I \in \mathcal{I}$, with the dimension strictly lower than n . By using the Lie derivative for (17), each \mathcal{C}_I , $I \in \mathcal{I}$ can be expressed as

$$\mathcal{C}_I = \left\{ x \in \mathbb{R}^n \mid \begin{array}{l} g_I x + b_I = 0 \\ g_I(D_i x + d_i) = 0 \\ g_I D_i(D_i x + d_i) = 0 \\ \vdots \\ g_I D_i^{n-1}(D_i x + d_i) = 0 \\ H_i x + h_i \leq 0 \\ \text{and } \exists i, j \in I \text{ s.t. } D_i \neq D_j \end{array} \right\} \forall i \in I \quad (18)$$

The non-emptiness of each \mathcal{C}_I can be determined by checking the feasibility of a linear program.

Remark 3. Proposition 1 implies that the sensitivity Q_A is uniquely defined as long as the state does not remain on a cell boundary for any time interval, but always “passes through”. An important fact indicated by Proposition 1 is that the non-existence of $\frac{\partial \phi_b(x_0, \tau)}{\partial x_0}$ does not necessarily occur on the boundary of the PWA system; rather, it can also take place in the interior of any polyhedron \mathcal{R}_i . The following example illustrates the set \mathcal{C} and also the set of initial states at which $\frac{\partial \phi_b(x_0, \tau)}{\partial x_0}$ fails to exist.

Example 1. Consider a two-dimensional PWA system illustrated in Fig. 2. The system is partitioned by three lines: $x_1 = 0$, $x_1 = 2$, and $x_2 = 0$, resulting in six polyhedra. The critical set \mathcal{C} , according to (18), consists of the positive segment of the x_1 -axis. For every initial point along the red and blue lines, when the trajectory ϕ_b reaches the right-half plane, it lacks a well-defined Jacobian. To prove this, we first note that for any initial state \bar{x}_0 starting from the red

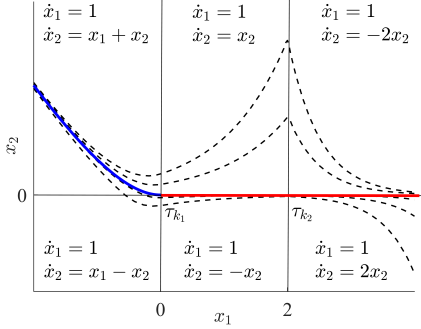


Fig. 2: The evolution of the PWA system given in Example 1. The black solid lines refer to the boundaries of the polyhedra. The critical set \mathcal{C} is the positive part of the x_1 -axis, represented by the red line. The backward reachable set $\Phi_{\text{back}}(\mathcal{C})$ is the union of the red and blue lines. According to Proposition 1, the solution ϕ_b is not differentiable at all points on the red and blue lines. The black dashed curves represent some trajectories starting near the blue line.

line (\mathcal{C}) , the solution will always remain in \mathcal{C} . Therefore, $\Phi_{\text{for}}(\bar{x}_0) \cap \mathcal{C} \neq \emptyset$, and $\frac{\partial \phi_b(x_0, \tau)}{\partial x_0}$ does not exist, according to Proposition 1. Then, we analyze the initial states in the first quadrant. By solving the affine system in this quadrant, we get the evolution: $x_1(\tau) = x_1(0) + \tau$, $x_2(\tau) = (x_1(0) + x_2(0) + 1)e^\tau - \tau - x_1(0) - 1$, for $\tau \geq 0$ such that $x_1(\tau) \leq 0$ and $x_2(\tau) \geq 0$. If $\Phi_{\text{for}}(\bar{x}_0) \cap \mathcal{C} \neq \emptyset$, at a certain time instant τ_{k_1} it must hold that $x_1(\tau_{k_1}) = x_2(\tau_{k_1}) = 0$. Otherwise, the trajectory can only converge to the red line asymptotically. From $x_1(\tau_{k_1}) = x_2(\tau_{k_1}) = 0$, we can derive the relation:

$$x_2(0) = e^{x_1(0)} - x_1(0) - 1. \quad (19)$$

The blue line corresponds to (19) in the first quadrant.

By simulating the system starting from the points near the blue line, we can find that even a small perturbation on the initial state will result in a large gap when the trajectory goes into the right-half plane. This validates that the classical Jacobian does not exist at the initial states on the blue curve after the critical time when the trajectory enters the red line.

The sensitivity branches at the time τ when the solution $\phi_b(x_0, \tau)$ enters the critical set \mathcal{C} . Fig. 3 gives a geometric interpretation of $Q_A(x_0, \tau)$.

C. Equivalence between $\text{conv}(Q_A)$ and $\partial_C \phi_b$

In this subsection, we show that $\text{conv}(Q_A(x_0, \tau)) = \partial_C \phi_b(x_0, \tau)$, $\forall x_0 \in \mathbb{R}^n$ and $\forall \tau \in [0, \infty)$. Toward this end, the following lemma and assumption are useful.

Lemma 3. Consider the PWA system (10) and its Aumann sensitivity Q_A defined in (15). For any $x_0 \in \mathbb{R}^n$, any $\tau \in [0, \infty)$, and any $Q(x_0, \tau) \in Q_A(x_0, \tau)$, $Q(x_0, \tau)$ is invertible.

Proof. According to (16), any $Q(x_0, \tau)$ can be recursively

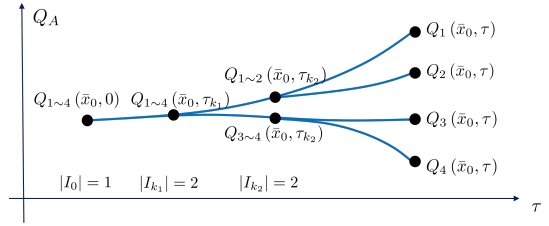


Fig. 3: Evolution of the sensitivity function Q_A over time for any initial state at the blue line in Fig. 2. The components Q_1 to Q_4 represent individual elements of Q_A . The sensitivity branches when the solution $\phi_b(\bar{x}_0, \tau)$ enters each critical set. In Example 1, this occurs at τ_{k_1} when the trajectory reaches $(0, 0)$ and at τ_{k_2} when the trajectory reaches $(2, 0)$.

computed by

$$Q(x_0, t) = \begin{cases} e^{D_{i_0} \tau}, \tau \in [\tau_0, \tau_1) \\ e^{D_{i_1}(\tau - \tau_1)} Q(x_0, \tau_1), t \in [\tau_1, \tau_2) \\ \dots \\ e^{D_{i_{M-1}}(\tau - \tau_{M-1})} Q(x_0, \tau_{M-1}), \tau \in [\tau_{M-1}, \tau_M), \end{cases} \quad (20)$$

where $\{i_0, i_1, \dots, i_M\} \in I(x_0)$ and $I(x_0)$ is the Cartesian product of the switching sequence $\{I_0, I_1, \dots, I_M\}$ for given x_0 .

As $e^{D_{i_0} \tau}$ is always invertible, and AB is invertible for any two invertible matrices A and B , it is straightforward to prove by induction that $Q(x_0, \tau)$ is invertible for any $x_0 \in \mathbb{R}^n$ and $\tau \in [0, \infty)$. \square

Assumption 2. For any $x_0 \in \Phi_{\text{back}}(\mathcal{C})$, any $\tau \in [0, \infty)$, and any $Q(x_0, \tau) \in \text{conv}(Q_A(x_0, \tau))$, $Q(x_0, \tau)$ is invertible.

Remark 4. Since any $Q \in Q_A$ is invertible according to Lemma 3, we further assume that any element in the convex hull of Q_A is invertible. Although convex combinations may not preserve invertibility, Assumption 2 is typically satisfied in practical scenarios such as adaptive cruise control with PWA models in [41] and the inverted pendulum system considered in [22] and the case study of the current paper. This assumption is crucial in the subsequent analysis on the equivalence between $\text{conv}(Q_A)$ and $\partial_C \phi_b$, as it enables the application of the inverse function theorem [35, Theorem 1] for the non-smooth solution ϕ_b .

Proposition 2. Consider the PWA system (10) and its two generalized sensitivities Q_A and $\partial_C \phi_b$. Suppose Assumption 2 holds. We have $\text{conv}(Q_A(x_0, \tau)) = \partial_C \phi_b(x_0, \tau)$, $\forall x_0 \in \mathbb{R}^n$ and $\forall \tau \in [0, \infty)$.

Proof. See Appendix C. \square

Proposition 2 indicates that the convex hull of the Aumann sensitivity, computed via (16) can replace the Clarke sensitivity in the formulation of the proposed PSF (11).

D. Implementation of the all-elements PSF

Problem (11) is a semi-infinite programming problem [42, Chapter 5.4], i.e., it contains infinitely many constraints. To solve it, we adopt the following three steps.

Step 1: Transforming the constraints. Under the equivalence between $\partial_C \phi_b$ and $\text{conv}(Q_A)$, we replace $\partial_C \phi_b$ with $\text{conv}(Q_A)$ in the formulation (11) of the proposed all-elements PSF. In other words, in (11b) and (11c), the CBF constraints should be satisfied for any $Q \in \text{conv}(Q_A)$.

We first eliminate the infinite number of constraints stemming from the set-valued generalized Clarke derivatives. Since (i) the CBF constraints are linear in h_X , h_b , and Q , and (ii) the sets $\partial_C h_X$, $\partial_C h_b$, and $\text{conv}(Q_A)$ are convex, according to [43, Proposition 2.1], (11b) and (11c) are equivalent to

$$\begin{aligned} \partial h_X Q f_{\text{PWA}}(x, u) &\geq -\alpha(h_X(\phi_b(x, \tau))), \\ \forall \partial h_X \in J_{h_X}(\phi_b(x, \tau)), \forall Q \in Q_A(x, \tau), \forall \tau \in [0, T], \\ \partial h_b Q f_{\text{PWA}}(x, u) &\geq -\alpha_b(h_b(\phi_b(x, T))), \\ \forall \partial h_b \in J_{h_b}(\phi_b(x, T)), \forall Q \in Q_A(x, T), \end{aligned} \quad (21)$$

where $J_{h_X}(\phi_b(x, \tau)) =$

$$\left\{ \lim_{i \rightarrow \infty} D h_X(y_i) \mid y_i \rightarrow \phi_b(x, \tau), h_X \text{ is differentiable at } y_i \right\}$$

and J_{h_b} is defined similarly to J_{h_X} . According to Definition 3, the set-valued functions J_{h_b} and J_{h_X} denote the collections of limiting derivatives that generate $\partial_C h_b$ and $\partial_C h_X$, respectively, i.e., $\partial_C h_b(\phi_b(x, T)) = \text{conv}(J_{h_b}(\phi_b(x, T)))$ and $\partial_C h_X(\phi_b(x, \tau)) = \text{conv}(J_{h_X}(\phi_b(x, \tau)))$.

Note that J_{h_b} and J_{h_X} are in general computable, as the explicit expressions of h_b and h_X are usually known. Besides, the Aumann sensitivity Q_A is computed through (16). Note that $|J_{h_b}|$, $|J_{h_X}|$, and $|Q_A|$ are finite.

Step 2: Mixed-integer encoding of f_{PWA} . Mixed-integer encoding is commonly used in hybrid MPC in which the PWA prediction model is usually converted into an equivalent mixed-logical dynamical form [3].

If the partition of the PWA system (9) is only in the state space, i.e., $f_{\text{PWA}}(x, u) := A_i x + B_i u + c_i$, for $x \in \mathcal{P}_i$, the inequalities in (21) are naturally linear in u and hence there is no need to do mixed-integer encoding.

If the partition is in both state and input spaces, to make the inequalities in (21) linear in u , we follow [13] to use the Big-M approach to get the equivalent mixed-integer formulation of $f_{\text{PWA}}(x, u)$, which is given by

$$f_{\text{PWA}}(x, u) = \sum_{i=1}^p f_i, \sum_{i=1}^p \Delta_i = 1$$

$$\text{for } i = 1, 2, \dots, p : \begin{cases} f_i \leq \bar{M} \Delta_i \\ f_i \geq \underline{M} \Delta_i \\ f_i \leq A_i x + B_i u + c_i - \underline{M} (1 - \Delta_i) \\ f_i \geq A_i x + B_i u + c_i - \bar{M} (1 - \Delta_i) \\ \Psi_i^{(x)} x + \Psi_i^{(u)} u \leq \psi_i + \bar{M}_i^* (1 - \Delta_i), \end{cases} \quad (22)$$

where the matrices $\Psi_i^{(x)}$, $\Psi_i^{(u)}$, and ψ_i constitute the hyperplane representation $\{[x^T, u^T]^T \in \mathbb{R}^{n+m} \mid \Psi_i^{(x)} x + \Psi_i^{(u)} u \leq \psi_i\}$ of the polyhedral region \mathcal{P}_i in (9), \bar{M} , \underline{M} , and \bar{M}_i^* are some bounds of affine functions $A_i x + B_i u + c_i$ and $\Psi_i^{(x)} x + \Psi_i^{(u)} u - \psi_i$ over $X \times U$. The detailed expressions of these bounds are provided in [13]. Besides, $\Delta_i \in \{0, 1\}$, $i = 1, 2, \dots, p$ are binary variables.

Step 3: Discretizing the time τ . After Steps 1 and 2, the infinite number of constraints in (21) comes only from the continuous time set $[0, T]$. In practice, to obtain computational tractability, the constraints are usually relaxed into a finite number of constraints that should be satisfied at some time instants [24]. In particular, given the prediction horizon $T > 0$ and a number $N \in \mathbb{N}^+$, the time set $[0, T]$ is discretized into $\{\tau_{(l)}\}_{l=0}^N$, where each $\tau_{(l)} = lT/N$. As a result, (21) is relaxed into an inequality constraint that should be satisfied at finitely many $\tau_{(l)}$.

After applying the three steps above, problem (11) becomes a convex QP if the PWA system (9) is partitioned only over the state space. If the partition is defined over the joint state-input space, the problem (11) typically becomes an MIQP.

V. EXPLICIT APPROXIMATION OF THE SAFE CONTROLLER

In the previous section, we have shown that the intractable constraints in (11) can be reformulated using Aumann sensitivity. However, When the partition of the PWA system (9) is defined over the joint state-input space, the computation time for solving the MIQP derived from (11) in practice grows dramatically with the number of binary variables in the worst case [44]. The number of binary variables itself scales linearly with the number p of regions. Consequently, the proposed all-elements PSF becomes impractical for real-time control systems with limited computational resources. To address this challenge (Problem 3), we further derive an explicit approximation for the solution to (11). This explicit solution is guaranteed to be feasible w.r.t. (11) if the original problem is feasible, and can be computed efficiently.

Our design is inspired by [45], where a constrained neural network is employed to approximate solutions of convex constrained optimization problems. An important property of (11) we use is that the backup solution $\pi_b(x)$ is a feasible solution to (11) for any $x \in \Phi_{\text{const}}(S_b, T)$, as has been proved in Theorem 1.

For each x , define by $U_{(11)}(x)$ the feasible set of (11). First, we restrict the constraint on u from u belonging to the whole feasible set $U_{(11)}(x)$ to

$$u \in U_{(11)}(x) \cap U_{\text{line}}(x), \quad (23)$$

where $U_{\text{line}}(x)$ is the line segment with the endpoints $\pi_b(x)$ and $\pi_r(x)$. Mathematically, $U_{\text{line}}(x) = \{u \in \mathbb{R}^m \mid u = \pi_b(x) + \lambda(\pi_r(x) - \pi_b(x)), \lambda \in [0, 1]\}$.

By adding the constraint $u \in U_{\text{line}}(x)$ into the optimization problem (11), we obtain that the optimizer $\hat{\pi}_{\text{safe}}(\cdot) : \mathbb{R}^n \rightarrow \mathbb{R}^m$ of the modified problem takes the following form:

$$\hat{\pi}_{\text{safe}}(x) = \pi_b(x) + \lambda^*(x)(\pi_r(x) - \pi_b(x)), \quad (24)$$

where

$$\begin{aligned} \lambda^*(x) &= \max_{\lambda \in [0, 1]} \lambda \\ \text{s.t. } u &= \pi_b(x) + \lambda(\pi_r(x) - \pi_b(x)), u \in U_{(11)}(x). \end{aligned} \quad (25)$$

Since each polyhedral region \mathcal{P}_i has the hyperplane representation $\{[x^T, u^T]^T \in \mathbb{R}^{n+m} \mid \Psi_i^{(x)} x + \Psi_i^{(u)} u \leq \psi_i\}$, for any

state x , we can determine the slice $U_i(x)$ of \mathcal{P}_i , defined by

$$U_i(x) := \{u \in \mathbb{R}^m \mid \Psi_i^{(u)} u \leq \psi_i - \Psi_i^{(x)} x\}. \quad (26)$$

Let $I_u(x)$ denote the set of indices i for which $U_i(x)$ is not empty. By substituting the expression of f_{PWA} into (11) and applying Step 1 of Section IV-D, we can rewrite the optimizer λ^* in a more compact form:

$$\begin{aligned} \lambda^*(x) &= \max_{\lambda} \lambda \\ \text{s.t. } &\exists i \in I_u(x) \text{ s.t. } \eta_i(x, \tau) \lambda \leq \omega_i(x, \tau), \forall \tau \in [0, T], \end{aligned} \quad (27)$$

where η_i and ω_i are vector-valued functions with proper dimensions. The expressions of η_i and ω_i can be obtained based on (9), (21), and (25). To derive the explicit form of λ^* , the constraint $\lambda \in [0, 1]$ is incorporated in (27) with the form of $[1 \ -1]^T \lambda \leq [1 \ 0]^T$.

The following proposition gives the explicit form of the optimizer λ^* .

Proposition 3. Consider the optimization problem (25) or (27), the optimizer λ^* has the expression:

$$\lambda^*(x) = \max_{i \in I_u(x)} \min_{\tau \in [0, T]} \min_{j \in \mathbb{N}_{\dim(\eta_i)}^+} \lambda_{i,j}(x, \tau), \quad (28)$$

with

$$\begin{aligned} &\lambda_{i,j}(x, \tau) \\ &= \begin{cases} \frac{\omega_{i,j}}{\eta_{i,j}}, & \text{if } \eta_{i,j} > 0 \\ \text{step}(\omega_{i,j}), & \text{if } \eta_{i,j} = 0 \\ \text{step} \left(\omega_{i,j} - \eta_{i,j} \min_{\lambda_{i,j'}(x, \tau') \in (0, 1)} \lambda_{i,j'}(x, \tau') \right), & \text{if } \eta_{i,j} < 0, \end{cases} \end{aligned} \quad (29)$$

where $\omega_{i,j}$ and $\eta_{i,j}$ represent the j -th element of ω_i and η_i , respectively, and we omit their dependence on x and τ for notational brevity.

Proof. See Appendix D. \square

Since $\hat{\pi}_{\text{safe}}$ is a feasible solution to the proposed all-elements PSF (11), we immediately have the following corollary of Theorem 2 and Proposition 3 on the safety performance of $\hat{\pi}_{\text{safe}}$:

Corollary 1. Consider the continuous PWA system (9) and the proposed all-elements PSF (11). Suppose that Assumptions 1 and 2 hold and that the approximate policy $\hat{\pi}_{\text{safe}}$ in (24) with λ^* computed from (28) is locally Lipschitz continuous. Then, the approximate policy $\hat{\pi}_{\text{safe}}$ renders $\Phi_{\text{const}}(S_b, T)$ forward invariant.

Akin to Step 3 of Section IV-D, implementing the approximate policy (24) needs the discretization of the time set $[0, T]$ appearing in (28).

Remark 5. Unlike [45], which computes explicit approximations for convex optimization problems, our approach accommodates non-convex MIQPs. Compared to our previous work [46], which also finds explicit approximations for MIQP problems, we extend the framework to problems with infinitely many constraints.

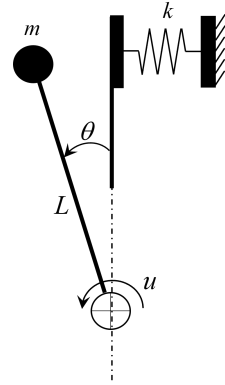


Fig. 4: Diagram of the inverted pendulum interacting with an elastic wall.

VI. CASE STUDIES

A. Inverted pendulum

To demonstrate the theoretical results, control of a simple inverted pendulum that interacts with an elastic wall (illustrated in Fig. 4) is considered. The system is linearized around the upright position, resulting in the following PWA system:

$$\ddot{\theta} = \begin{cases} \frac{g}{L} \theta + \frac{1}{mL^2} u, & \text{if } \theta \geq 0 \\ \left(\frac{g}{L} - kL \right) \theta + \frac{1}{mL^2} u, & \text{if } \theta < 0, \end{cases}$$

where θ is the pendulum angle, u is the input torque, the state variable $x = [\theta \ \dot{\theta}]^T$, $m = 1$ kg, $L = 1$ m, $g = 10$ m/s², and $k = 2$ N/m is the spring of the wall. The state constraint is $x \in X := \{x \mid |\theta| \leq 0.5, |\dot{\theta}| \leq 2\}$, and the input constraint is $|u| \leq 10$. In the simulation, the system is discretized by forward Euler with a sampling time of 0.001 seconds.

The backup policy is designed as a linear feedback controller, given by $\pi_b(x) = -12\theta - 3\dot{\theta}$. Under this policy, the resulting PWA system takes the form:

$$\dot{x} = f_{\text{PWA},b}(x) = \begin{cases} \begin{bmatrix} 0 & 1 \\ -2 & -3 \end{bmatrix} x, & \text{if } x_1 \geq 0 \\ \begin{bmatrix} 0 & 1 \\ -4 & -3 \end{bmatrix} x, & \text{if } x_1 < 0. \end{cases} \quad (30)$$

The feedback gain $[-12 \ -3]$ is selected such that both linear modes of (30) are Hurwitz stable.

According to Proposition 1, $x = [0 \ 0]^T$ is the only initial point at which the Aumann sensitivity contains multiple (two in this case) elements. Under the backup policy, a quadratic CBF $h_b(x) = \gamma - x^T R x$ is synthesized using the LMI approach presented in [7]. The reference control policy is chosen as $\pi_r(x) = -12(\theta - \theta_r) - 3(\dot{\theta} - \dot{\theta}_r) + mL^2 \ddot{\theta}_r - mgL \theta_r$, which is a proportional-derivative plus feedforward controller. The reference angle $\theta_r(t) = 0.8 \cos(t)$. This means that during some periods, the reference state violates the state constraint. For the PSF in (11), the horizon T is set to 1 second and $[0, T]$ is further discretized into $N = 50$ intervals, resulting in the time grid $\{iT/N\}_{i=0}^N$.

Fig. 5 compares the time responses of the closed-loop system under the PSF (11) and the standard safety filter using

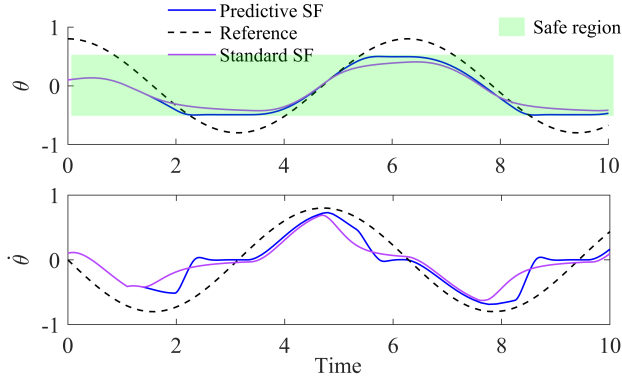


Fig. 5: Time responses of the closed-loop system with the PSF (11) and the standard safety filter. The initial state is $[0.1 \ 0.1]^T$. “SF” means “safety filter”. Both SFs successfully control the system without recording any constraint violations. The predictive SF is less conservative than the standard SF because the trajectory regulated by the predictive SF is closer to the reference.

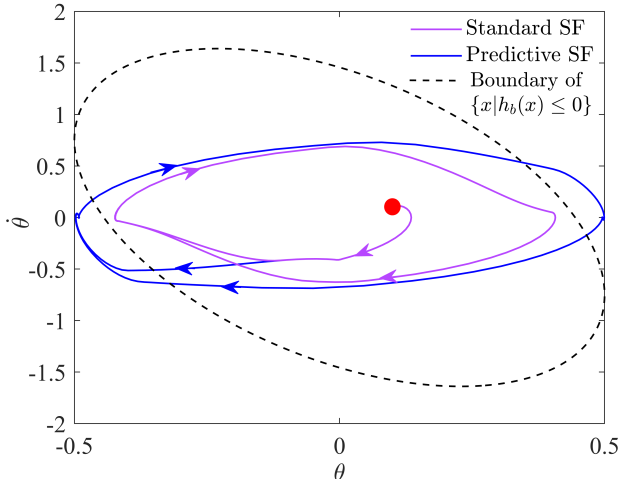


Fig. 6: Trajectories of the closed-loop system (solid lines) and the safe set of h_b (black dashed line). The black hole represents the initial state. By virtue of predictions, the predictive SF enlarges the original feasible region $\{x|h_b(x) \leq 0\}$.

the CBF h_b without predictions. The initial state is $[0.1 \ 0.1]^T$. From Fig. 5, it is observed that even though the reference state violates the state constraint, the trajectories controlled by these two safety filters always satisfy the state constraint. As evidenced by the first and third sub-figures, the PSF is less conservative because the corresponding trajectory stays closer to the reference. Furthermore, Fig. 6 displays the trajectories and also the safe set of h_b . It is found that the feasible region of the PSF exceeds the boundary of the safe set of h_b (i.e., the feasible region of the standard safety filter), highlighting the superiority of the predictive approach over the standard method.

Next, we examine a scenario in which the PSF based on the classical gradient (7) fails to ensure safety. Consider the initial state $x(0) = [0.5 \ -2]^T$, which lies on the boundary of X . The

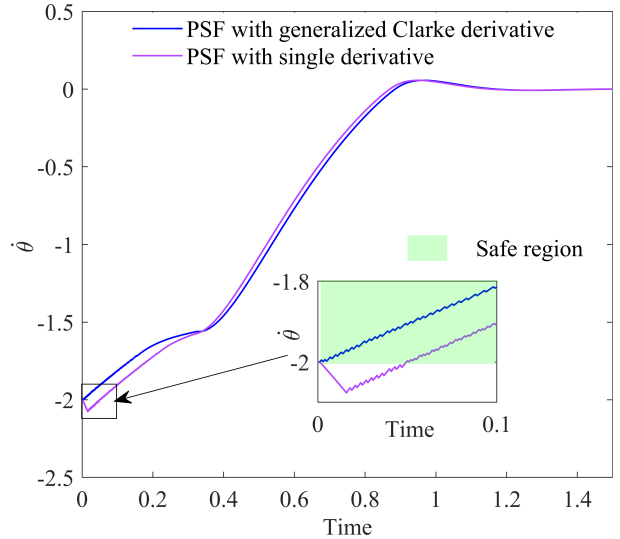


Fig. 7: Comparison of PSFs using generalized Clarke derivative and single derivative methods. The highlighted inset zooms into the initial phase of the trajectory, illustrating the difference in early behavior between the two methods. When the initial state is at the boundary of the state constraint set, the proposed all-elements PSF using generalized Clarke derivative successfully avoids the unsafe region. The classical PSF proposed in [9], [10] fails because of the mismatch in calculating the derivative of h_X , which arises from its non-smooth nature.

function h_X , defined as $h_X(x) := \min\{0.5 - \theta, \theta + 0.5, 2 - \dot{\theta}, \dot{\theta} + 2\}$, is not differentiable at $x(0)$. We design two PSFs: the first is based on (11), and the second is a modified version of (11) that includes only a single, randomly selected gradient from $\partial_C h_X$. The second one corresponds to the classical PSF, which implicitly assumes that h_X is differentiable everywhere. To highlight the difference between the two safety filters, a constant reference policy is chosen as $\pi_r(x) = -10$.

Fig. 7 illustrates the closed-loop trajectory of $\dot{\theta}$ under both safety filters. It is evident in the zoomed figure that the proposed all-elements PSF using the generalized Clarke derivative (blue curve) drives the system to remain within the safe region, while the safety filter using the single gradient (purple curve), proposed in [9], [10], experiences constraint violations during the initial phase⁵.

B. Temperature control

To demonstrate the computational advantage of the proposed explicit solution, we further consider a more complex PWA system with more partitions. In particular, let us consider control of the temperatures $x = [T_1 \ T_2 \ T_3 \ T_4]^T$ of four rooms in a building. The layout of the four rooms and heat flows are shown in Fig. 8.

The ambient temperature T_0 outside the building is assumed to be constantly zero, i.e., $T_0 = 0^\circ\text{C}$. Heat flows occur be-

⁵When the filter becomes infeasible, we switch to applying the reference π_r through a saturation unit $\max\{\min\{\cdot, 10\}, -10\}$, which enforces only the input constraint.

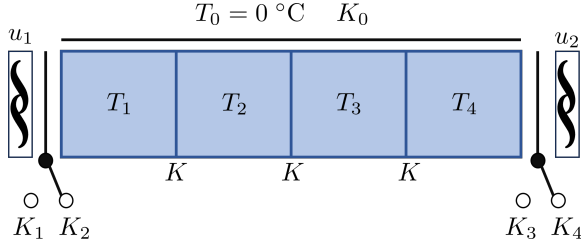


Fig. 8: Diagram of the building.

tween each two adjacent rooms as well as between the external environment and each room. These thermal interactions are modeled using linear equations. For example, the temperature dynamics in Room 2 are given by $\dot{T}_2 = K(T_1 - T_2) + K(T_3 - T_2) + K_0(T_0 - T_2)$, where the coefficients K and K_0 are the ratios of the corresponding thermal capacitance to thermal resistance. Room 1 and Room 4 are each equipped with a temperature controller (u_1 and u_2) to regulate the temperature in the respective room. We assume that the heaters are powerful enough such that they realize the demanded temperature values u_1 and u_2 immediately. The heat flow between a room and its controller is modeled by a piecewise linear equation. In particular, when the temperature difference $|u_1 - T_1|$ exceeds a threshold of 5°C , the system automatically switches to a mode with a larger coefficient $K_2 > K_1$ to facilitate better heat conduction. To summarize, the system admits the following state space equation:

$$\begin{aligned}\dot{T}_1 &= \begin{cases} K(T_2 - T_1) + K_1(u_1 - T_1) + K_0(T_0 - T_1), & \text{if } |u_1 - T_1| \leq 5 \\ K(T_2 - T_1) + K_2(u_1 - T_1) + K_0(T_0 - T_1), & \text{otherwise} \end{cases} \\ \dot{T}_2 &= K(T_1 - T_2) + K(T_3 - T_2) + K_0(T_0 - T_2) \\ \dot{T}_3 &= K(T_2 - T_3) + K(T_4 - T_3) + K_0(T_0 - T_3) \\ \dot{T}_4 &= \begin{cases} K(T_3 - T_4) + K_3(u_2 - T_4) + K_0(T_0 - T_4), & \text{if } |u_2 - T_4| \leq 5 \\ K(T_3 - T_4) + K_4(u_2 - T_4) + K_0(T_0 - T_4), & \text{otherwise,} \end{cases}\end{aligned}$$

where $K = 0.0035 \text{ s}^{-1}$, $K_0 = 0.001 \text{ s}^{-1}$, $K_1 = 0.01 \text{ s}^{-1}$, $K_2 = 0.02 \text{ s}^{-1}$, $K_3 = 0.008 \text{ s}^{-1}$, and $K_4 = 0.016 \text{ s}^{-1}$. This PWA system can be rewritten as the standard form of (9), with a total of 9 polyhedral regions.

The control objective is to adjust the temperatures of Room 2 and Room 3 to 20°C , while keeping the temperatures of Room 1 and Room 4 no higher than 26°C . The input constraints are given by $u_1, u_2 \in [-10, 35]$. The initial state is $[5 \ 20 \ 10 \ 15]^T$. In the simulation, the system is discretized using the forward Euler method with a sampling time of 1 second.

The reference controller is designed based on backstepping [33, Chapter 14.3]. In particular, to make T_2 and T_3 track 20°C , a virtual controller v for T_1 and T_4 is designed as

$$v = K_{23}^u \left(\begin{bmatrix} T_2 \\ T_3 \end{bmatrix} - \begin{bmatrix} 20 \\ 20 \end{bmatrix} \right) - B_{23}^{-1} A_{23} \begin{bmatrix} 20 \\ 20 \end{bmatrix}$$

where A_{23} and B_{23} are the system matrices of the linear sub-equations for \dot{T}_2 and \dot{T}_3 , where T_2 and T_3 are the states and T_1 and T_4 are the inputs. The feedback gain K_{23}^u is chosen as the LQR gain for the linear subsystem with $Q = I_2$ and $R = I_2$. The second term of v is a feedforward term. Then,

the real reference input is determined by

$$\pi_r(x) = K_{14}^u \left(\begin{bmatrix} T_1 \\ T_4 \end{bmatrix} - v \right) - B_{14}^{-1} A_{14} v - \begin{bmatrix} T_2 K / K_1 \\ T_3 K / K_3 \end{bmatrix}$$

where A_{14} and B_{14} are the system matrices of the linear subsystem for T_1 and T_4 , corresponding to the region where $|u_1 - T_1| \leq 5$ and $|u_2 - T_4| \leq 5$, with T_2 and T_3 treated as external disturbances. The feedback gain K_{14}^u is designed similarly to K_{23}^u . The second term of π_r is a feedforward term, while the third term compensates for the external disturbances.

Now, consider the backup CBF candidate $h_b(x) = \min\{24 - T_1, 24 - T_4\}$. It can be verified that by choosing the backup controller $\pi_b(x) = \begin{bmatrix} -KT_2 / K_1 \\ -KT_3 / K_3 \end{bmatrix}$, h_b satisfies $\partial h_b f_{\text{PWA},b}(x) \geq -\alpha_b h_b(x)$, $\forall x \geq [0 \ 0 \ 0 \ 0]^T$, $\forall \partial h_b \in \partial_C h_b(x)$ and $\forall \alpha_b \in (0, K + K_0 + \max\{K_1, K_3\})$. Here $f_{\text{PWA},b}$ represents the system (31) controlled by π_b . The above analysis indicates that h_b and π_b are valid, i.e., satisfy Assumption⁶ 1.

Fig. 9 plots the time responses of the closed-loop system controlled by $\hat{\pi}_{\text{safe}}$ and π_{safe} . The PSF (11) is implemented over a prediction horizon of $T = 4$ seconds, which is discretized into $N = 40$ uniformly spaced time steps. This corresponds to a discretization interval of 0.1 seconds. From the top-left and bottom-right sub-figures, it is observed that all the controllers satisfy the safety requirements ($T_1, T_4 \leq 26^\circ\text{C}$). On the other hand, the top-right and bottom-left sub-figures show that both $\hat{\pi}_{\text{safe}}$ and π_{safe} with $N = 40$ drive the temperatures T_2 and T_3 closer to the target temperature (20°C), compared to $\hat{\pi}_{\text{safe}}$ and π_{safe} with $N = 0$ (i.e., policies derived from a standard CBF-based safety filter without predictions). Furthermore, consistent with intuition, the approximate explicit policy $\hat{\pi}_{\text{safe}}$ has a slightly worse tracking performance than the exact one π_{safe} , as evidenced by the red and blue curves in the top-right and bottom-left sub-figures.

In Fig. 10, we compare the tracking performance and average CPU time of the controller π_{safe} and its explicit approximation $\hat{\pi}_{\text{safe}}$ for different prediction horizons. The tracking performance is defined as the summation of $(T_2 - 20)^2 + (T_3 - 20)^2$ over 2000 seconds. To implement π_{safe} , according to Section IV-D, an MIQP problem needs to be solved online. The results show that the approximate controller $\hat{\pi}_{\text{safe}}$ retains a comparable tracking performance to the exact one π_{safe} , and the average CPU time for $\hat{\pi}_{\text{safe}}$ (red line) is 1–2 orders of magnitude lower than that for the exact policy π_{safe} (blue line) across all prediction horizons, highlighting the practicality of the approximation in real-time or resource-constrained settings. Meanwhile, increasing the prediction horizon leads to reduced tracking errors for both $\hat{\pi}_{\text{safe}}$ and π_{safe} , while their CPU times grow approximately linearly. This demonstrates that incorporating predictions can effectively reduce the conservatism of the safety filter, compared to a standard CBF-based approach without predictions.

⁶Strictly speaking, Assumption 1 is not completely satisfied because the inequality in condition (ii) holds only for $x \geq [0 \ 0 \ 0 \ 0]^T$ in this example. However, this does not pose a problem as long as the system operates within the positive state region.

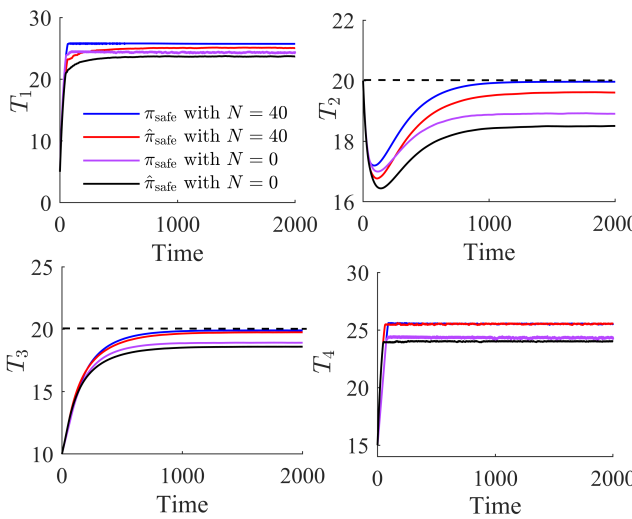


Fig. 9: Time responses of the closed-loop system controlled by $\hat{\pi}_{\text{safe}}$ and π_{safe} . The black dashed lines represent the target temperature. The policy with $N = 40$ is derived from (11) with the prediction horizon $T = 4$ seconds and discretized into $N = 40$ uniformly spaced time steps. The policy with $N = 0$ is derived from a standard CBF-based safety filter without any predictions. Both $\hat{\pi}_{\text{safe}}$ and π_{safe} with $T = 4$ drive the temperatures T_2 and T_3 closer to the target temperature (20°C), compared to $\hat{\pi}_{\text{safe}}$ and π_{safe} with $N = 0$. As expected, the approximate explicit policy $\hat{\pi}_{\text{safe}}$ exhibits a slightly worse tracking performance compared to the exact policy π_{safe} .

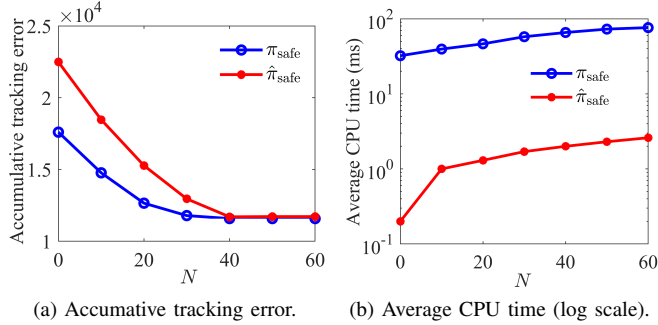


Fig. 10: Tracking performance and average CPU time (log scale) for different prediction horizons for the exact policy π_{safe} and the approximate policy $\hat{\pi}_{\text{safe}}$. The tracking errors (defined as the summation of $(T_2 - 20)^2 + (T_3 - 20)^2$ over 2000 seconds) are comparable, but the approximate policy significantly reduces the computational cost by up to two orders of magnitude across all horizons.

VII. CONCLUSIONS AND FUTURE WORK

This paper has developed a novel predictive safety filter (PSF) to achieve less conservative control of constrained piecewise affine (PWA) systems compared to standard safety filters that use control barrier functions (CBFs) or projections onto invariant sets. We have extended the predictive CBF method to handle the non-smoothness occurring in PWA dynamics, in the state constraint, as well as in the CBF. We have further derived an explicit approximation of the solution to the PSF. Such an approximation can be efficiently computed through basic arithmetic and min/max operations. A case study on an inverted pendulum interacting with an elastic wall has shown improved safety performance compared to classical PSFs. Furthermore, simulations on temperature control of a building have demonstrated the computational advantages of the approximate solution.

In the future, we will consider designing PSFs for general Lipschitz continuous nonlinear systems and exploring their explicit approximation. The PSF method can be viewed as an online version of HJ reachability. We believe that unifying these two methods is a meaningful future research direction. Besides, another interesting topic is to consider probabilistic safety constraints under model uncertainties.

APPENDIX

A. Proof of Lemma 2

For the convenience of using the comparison theorem [33, Lemma 3.4], we define $\bar{h} = -h$. Since \bar{h} is not always differentiable, we consider the generalized directional derivative [47]

$$\bar{h}^\circ(x; v) := \limsup_{w \rightarrow 0, \delta \downarrow 0} \frac{\bar{h}(x + w + \delta v) - \bar{h}(x + w)}{\delta} \quad (31)$$

for any $v \in \mathbb{R}^n$. The generalized directional derivative is well-defined for Lipschitz continuous functions. According to [47, Proposition 1.4], we have

$$\bar{h}^\circ(x; v) = \max_{\partial \bar{h} \in \partial_C \bar{h}(x)} \{\partial \bar{h} v\}.$$

By specifying $v = f(x, \pi(x))$ and noting that $\partial_C \bar{h}(x) = -\partial \bar{h}(x)$ and that (12) holds, we have

$$\bar{h}^\circ(x; f(x, \pi(x))) = \max_{\partial \bar{h} \in \partial_C \bar{h}(x)} \{\partial \bar{h} f(x, \pi(x))\} \leq -\alpha(\bar{h}(x)), \quad \forall x \in \{x \in \mathbb{R}^n | \bar{h}(x) \leq 0\}. \quad (32)$$

Consider the upper right-hand time derivative of \bar{h} along $\dot{x} = f(x, \pi(x))$, which is defined by

$$D^+ \bar{h}(x_0, t) := \limsup_{\tau \downarrow 0} \frac{\bar{h}(\phi(x_0, t + \tau)) - \bar{h}(\phi(x_0, t))}{\tau}. \quad (33)$$

Since ϕ is the solution of the closed-loop system $\dot{x} = f(x, \pi(x))$, we have the relation $\phi(x_0, t) + \limsup_{w \rightarrow 0, \delta \downarrow 0} w + \delta f(\phi(x_0, t), \pi(\phi(x_0, t))) = \limsup_{\tau \downarrow 0} \phi(x_0, t + \tau)$. As a result, by comparing (31) and (33) and noting that (32) holds, we obtain

$$\begin{aligned} D^+ \bar{h}(x_0, t) &= \bar{h}^\circ(\phi(x_0, t), f(\phi(x_0, t), \pi(\phi(x_0, t)))) \\ &\leq -\alpha(\bar{h}(\phi(x_0, t))), \quad \forall t \geq 0 \end{aligned}$$

if $x_0 \in \{x \in \mathbb{R}^n \mid \bar{h}(x) \leq 0\}$. Because α is Lipschitz continuous, directly applying the comparison theorem [33, Lemma 3.4] yields $\bar{h}(\phi(x_0, t)) \leq 0, \forall t \geq 0$, which consequently proves Lemma 2.

B. Proof of Proposition 1

The equivalence between (3) and (4) follows from the definitions of backward and forward reachable sets. The equivalence between (1) and (2) stems from Definition 5.

If $\Phi_{\text{for}}(\bar{x}_0) \cap \mathcal{C} \neq \emptyset$, $\phi_b(\bar{x}_0, \tau)$ is on the boundary of multiple polyhedra of the PWA system (10) during $[\tau_k, \tau_{k+1})$, where $\{(\tau_0, I_0), (\tau_1, I_1), \dots, (\tau_M, I_M)\}$ constitutes the time-stamped switching sequence of the solution $\phi_b(\bar{x}_0, \tau)$. To see why this is true, note that if $\Phi_{\text{for}}(\bar{x}_0) \cap \mathcal{C} \neq \emptyset$, there exists at least one instant $\tau_k \geq 0, k \in \mathbb{N}_M$ such that $\phi_b(\bar{x}_0, \tau_k) \in \mathcal{C}$. According to the definition of \mathcal{C} , $\bar{g}_{I_k}^{(q)}(x(\tau_k)) = g_{I_k} D_i^{q-1}(D_i x(\tau_k) + d_i) = 0, \forall q \in \mathbb{N}_n^+$. Using the Cayley–Hamilton Theorem [40], we know that $\bar{g}_{I_k}^{(q)}(x(\tau_k)) = 0, \forall q \in \mathbb{N}$, meaning that any order time derivative of \bar{g}_{I_k} vanishes when $\tau = \tau_k$. Consequently, \bar{g}_{I_k} remains zero during $[\tau_k, \tau_{k+1})$, $\tau_{k+1} > \tau_k$, i.e., the set Γ_I is an *invariant manifold* [33, Chapter 8.1], so the trajectory must stay in Γ_I over the time interval $[\tau_k, \tau_{k+1})$. We refer to all such intervals as *critical periods*. During these periods, ϕ_b resides at the intersection of the closure of multiple regions.

(3) \Rightarrow (2): If $\Phi_{\text{for}}(\bar{x}_0) \cap \mathcal{C} = \emptyset$, we can distinguish two cases. In the first case, there is no critical period. This means that for any switching instant τ_k , the trajectory crosses the hyperplane $\{x \in \mathbb{R}^n \mid \bar{g}_{I_k \cup I_{k+1}}(x) = 0\}$ from \mathcal{R}_{I_k} and immediately enters the interior of one of the intersecting polyhedra $\mathcal{R}_{I_{k+1}}$. Here, all I_k have only one element. When $\tau \in (\tau_k, \tau_{k+1})$, we know that $\partial f_{\text{PWA}, b}(\phi_b(\bar{x}_0, \tau))$ is uniquely determined by D_{I_k} . As a result, according to (16), $Q_A(\bar{x}_0, \tau)$ is single-valued.

In the second case of $\Phi_{\text{for}}(\bar{x}_0) \cap \mathcal{C} = \emptyset$, there still exists one or more critical periods during which $\bar{g}_{I_k}^{(q)} = 0, \forall q \in \mathbb{N}_n^+$. However, it must hold that $D_{i_k} = D_{j_k}$ for every two adjacent polyhedra \mathcal{R}_{i_k} and \mathcal{R}_{j_k} , $i_k, j_k \in I_k$. In this case $Q_A(\bar{x}_0, \tau)$ is still single-valued.

(2) \Rightarrow (3): We prove this implication by showing $\neg(3) \Rightarrow \neg(2)$. If $\Phi_{\text{for}}(\bar{x}_0) \cap \mathcal{C} \neq \emptyset$, according to the definition of \mathcal{C} , during each critical period $[\tau_k, \tau_{k+1})$, $\phi_b(\bar{x}_0, \tau)$ lies at the intersection of two or more adjacent polyhedra. As a result, the integral term of (16) admits at least two different forms $D_{i_k} Q(\bar{x}_0, s)$ and $D_{j_k} Q(\bar{x}_0, s)$, $i_k, j_k \in I_k$ from $s = \tau_k$ to $s = \tau_{k+1}$. By holding the integral term during the other periods $[\tau_0, \tau_1), \dots, [\tau_{k-1}, \tau_k), [\tau_{k+1}, \tau_{k+2}), \dots$ fixed, we know that $Q_A(\bar{x}_0, \tau)$ must take at least two different values for all $\tau > \tau_k$.

In addition, if \mathcal{C} is empty, then it follows from the above discussions that $\phi_b(x_0, \tau)$ has a global classical Jacobian w.r.t. x_0 .

C. Proof of Proposition 2

If $\phi_b(x_0, \tau)$ is differentiable w.r.t. x_0 at $x_0 = \bar{x}_0$, it is obvious that $\partial_C \phi_b(\bar{x}_0, \tau) = Q_A(\bar{x}_0, \tau) = \left. \frac{\partial \phi_b(x_0, \tau)}{\partial x_0} \right|_{x_0=\bar{x}_0}$. In the remainder of the proof, we consider the case when $Q_A(\bar{x}_0, \tau)$ has multiple values.

First, we prove $\partial_C \phi_b \subseteq \text{conv}(Q_A)$. For any \bar{x}_0 and τ such that $\phi_b(x_0, \tau)$ is not differentiable w.r.t. x_0 at $x_0 = \bar{x}_0$, consider any sequence $\{y_j\}_{j=0}^\infty$ satisfying $\lim_{j \rightarrow \infty} y_j = \bar{x}_0$ and that $\phi_b(x_0, \tau)$ is differentiable w.r.t. x_0 at y_j . Since y_j converges to \bar{x}_0 , there exists a sufficiently large $\bar{j} \in \mathbb{N}^+$ such that for any $j \geq \bar{j}$, $\phi_b(y_j, \tau)$ admits the same switching sequence $\{i_0, i_1, \dots, i_M\}$ satisfying $\{i_0, i_1, \dots, i_M\} \in I(\bar{x}_0)$, where $I(\bar{x}_0)$ is the Cartesian product of the switching sequence of $\phi_b(\bar{x}_0, \tau)$.

According to Definition 3, $\lim_{j \rightarrow \infty} J_{\phi_b}(y_j, \tau) \in \partial_C \phi_b(\bar{x}_0, \tau)$, where J_{ϕ_b} refers to the classical Jacobian and has the expression

$$J_{\phi_b}(y_j, \tau) = \begin{cases} e^{D_{i_0} \tau}, \tau \in [\tau_0, \tau_1) \\ e^{D_{i_1}(\tau - \tau_1)} J_{\phi_b}(y_j, \tau_1), \tau \in [\tau_1, \tau_2) \\ \dots \\ e^{D_{i_{M-1}}(\tau - \tau_{M-1})} J_{\phi_b}(y_j, \tau_{M-1}), \tau \in [\tau_{M-1}, \tau_M) \end{cases} \quad (34)$$

By comparing (20) and (34) and noting that the switching time τ_k is continuous to y_j , we can prove by induction that $\lim_{j \rightarrow \infty} J_{\phi_b}(y_j, \tau) = Q_{(i_0, i_1, \dots, i_M)}(\bar{x}_0, \tau) \in Q_A(\bar{x}_0, \tau)$. Here, the subscript (i_0, i_1, \dots, i_M) means that $Q_{(i_0, i_1, \dots, i_M)}$ corresponds to the element of Q_A that is determined by the switching sequence (i_0, i_1, \dots, i_M) . The containment of $\partial_C \phi_b$ in $\text{conv}(Q_A)$ follows from the arbitrariness of the sequence $\{y_j\}_{j=0}^\infty$.

Conversely, we prove $\text{conv}(Q_A) \subseteq \partial_C \phi_b$. Since we have proved that $\partial_C \phi_b \subseteq \text{conv}(Q_A)$, according to Assumption 2, any element of $\partial_C \phi_b$ is invertible. As a result, by virtue of the inverse function theorem for generalized Clarke derivatives [35, Theorem 1], we know that there exist a Lipschitz continuous function $\phi_b^{-1}(\cdot, \tau) : \mathbb{R}^n \rightarrow \mathbb{R}^n$, a neighborhood Y of \bar{x}_0 , and a neighborhood Z of $\phi_b(\bar{x}_0, \tau)$ such that $\phi_b^{-1}(\phi_b(y, \tau)) = y, \forall y \in Y$ and $\phi_b(\phi_b^{-1}(z, \tau)) = z, \forall z \in Z$.

Then, for any \bar{x}_0 and any τ such that $\phi_b(x_0, \tau)$ is not differentiable w.r.t. x_0 at $x_0 = \bar{x}_0$, consider any element $Q_{(i_0, i_1, \dots, i_M)}(\bar{x}_0, \tau)$ in $Q_A(\bar{x}_0, \tau)$. Note that $Q_{(i_0, i_1, \dots, i_M)}(\bar{x}_0, \tau)$ can be expressed by (20). Since ϕ_b is differentiable almost everywhere, we immediately know that $\Phi_{\text{back}}(\mathcal{C})$ has the dimension strictly lower than n . Therefore, we can always find a sequence $\{z_j\}_{j=1}^\infty$ satisfying $z_j \in Z, \forall j \in \mathbb{N}^+, z_j \notin \Phi_{\text{back}}(\mathcal{C}), \forall j \in \mathbb{N}^+$, and $\lim_{j \rightarrow \infty} z_j = \phi_b(\bar{x}_0, \tau)$. By substituting z_j to the inverse function ϕ_b^{-1} , we get a sequence $y_j = \phi_b^{-1}(z_j, \tau), j = 1, 2, \dots$. Thanks to the Lipschitz continuity of the inverse function, the sequence $\{y_j\}_{j=0}^\infty$ satisfies $\phi_b(y_j, \tau) = z_j, \lim_{j \rightarrow \infty} y_j = \lim_{j \rightarrow \infty} \phi_b^{-1}(z_j, \tau) = \bar{x}_0$, and $y_j \notin \Phi_{\text{back}}(\mathcal{C})$. As y_j converges to \bar{x}_0 , there exists a $\bar{j} \in \mathbb{N}^+$ such that for any $j \geq \bar{j}$, $\phi_b(y_j, \tau)$ admits the same switching sequence $\{i_0, i_1, \dots, i_M\} \in I(\bar{x}_0)$. As a result, $\lim_{j \rightarrow \infty} J_{\phi_b}(y_j, \tau) = Q_{(i_0, i_1, \dots, i_M)}(\bar{x}_0, \tau)$. It follows from Definition 3 that $Q_{(i_0, i_1, \dots, i_M)}(\bar{x}_0, \tau) \in \partial_C \phi_b(\bar{x}_0, \tau)$. This implies $\text{conv}(Q_A(\bar{x}_0, \tau)) \subseteq \partial_C \phi_b(\bar{x}_0, \tau)$, which completes the proof of Proposition 2.

D. Proof of Proposition 3

Let $\lambda^+(x)$ denote the right-hand side of (29). The proof is divided into two parts: proving the feasibility of $\lambda^+(x)$ and

the optimality of $\lambda^+(x)$.

(i) *Feasibility of $\lambda^+(x)$.* For any $x \in \Phi_{\text{const}}(S_b, T)$, since $\pi_b(x)$ is feasible for (11), 0 is feasible for (27) as well. Therefore, we know that $\exists i \in I_u(x)$ such that $\omega_{i,j}(x, \tau) \geq 0$, $\forall \tau \in [0, T]$ and $\forall j \in \mathbb{N}_{\dim(\eta_i)}^+$. Due to the maximization operator in (28), it further holds that $\lambda^+(x) \geq 0$.

Suppose without loss of generality that $\lambda^+(x) = \lambda_{i+,j+}(x, \tau^+)$ for a certain $i^+ \in I_u(x)$, $j^+ \in \mathbb{N}_{\dim(\eta_{i+})}^+$, and $\tau^+ \in [0, T]$. It follows from the two minimization operators in (28) that

$$\lambda^+(x) \leq \lambda_{i+,j}(x, \tau), \quad \forall j \in \mathbb{N}_{\dim(\eta_{i+})}^+ \text{ and } \forall \tau \in [0, T]. \quad (35)$$

Then, for any $j \in \mathbb{N}_{\dim(\eta_{i+})}^+$ and any $\tau \in [0, T]$, based on (29) we can distinguish the following four cases:

Case (1): $\eta_{i+,j}(x, \tau) > 0$. In this case, $\lambda_{i+,j}(x, \tau) = \frac{\omega_{i+,j}(x, \tau)}{\eta_{i+,j}(x, \tau)}$. Directly applying (35) yields

$$\eta_{i+,j}(x, \tau) \lambda^+(x) \leq \omega_{i+,j}(x, \tau). \quad (36)$$

Case (2): $\eta_{i+,j}(x, \tau) = 0$ and $\omega_{i+,j}(x, \tau) \geq 0$. In this case, (36) obviously holds.

Case (3): $\eta_{i+,j}(x, \tau) = 0$ and $\omega_{i+,j}(x, \tau) < 0$. From (29), we know that $\lambda_{i+,j}(x, \tau) = 0$, which further implies $\lambda^+(x) = 0$ because of (35) and $\lambda^+(x) \geq 0$. Consequently, the feasibility of $\lambda^+(x) = 0$ results from the feasibility of $\pi_b(x)$.

Case (4): $\eta_{i+,j}(x, \tau) < 0$. In this case, we only need to focus on the situation when $\lambda^+(x) > 0$ because if $\lambda^+(x) = 0$ then the feasibility of $\lambda^+(x)$ follows from the feasibility of $\pi_b(x)$. If $\lambda^+(x) > 0$, then by defining $\lambda_{i+}(x) := \min_{\tau' \in [0, T], j' \in \mathbb{N}_{\dim(\eta_{i+})}^+, \lambda_{i+,j'}(x, \tau') \in (0, 1)} \lambda_{i+,j'}(x, \tau')$, we have

$$\omega_{i+,j}(x, \tau) - \eta_{i+,j}(x, \tau) \lambda_{i+}(x) \geq 0. \quad (37)$$

Noticing the relation $\lambda^+(x) = \lambda_{i+,j+}(x, \tau^+) \geq \lambda_{i+}(x)$, we derive (36) from (37).

Combining the four cases above and noticing the arbitrariness of j and τ , we can conclude that $\lambda^+(x)$ satisfies the constraint of (27) for $i = i^+$. This proves the feasibility of $\lambda^+(x)$.

(ii) *Optimality of $\lambda^+(x)$.* If $\lambda^+(x) = 1$, the optimality follows directly from the constraint $\lambda \leq 1$. In the remainder of the proof, we consider $\lambda^+(x) < 1$ and prove that $\lambda^+(x) + \Delta_\lambda$ is infeasible for problem (27) for any $\Delta_\lambda \in (0, 1 - \lambda^+(x)]$. Since the objective of the optimization problem (25) is to maximize λ , the infeasibility of $\lambda^+(x) + \Delta_\lambda$ implies the optimality of $\lambda^+(x)$.

For any $i \in I_u(x)$, let $\lambda_i(x) = \lambda_{i,j^*}(x, \tau^*) := \min_{\tau \in [0, T]} \min_{j \in \mathbb{N}_{\dim(\eta_i)}^+} \lambda_{i,j}(x, \tau)$, and then we get the relation

$$\max_{i \in I_u(x)} \lambda_i(x) = \lambda^+(x) < 1. \quad (38)$$

Analogous to the proof of the feasibility, for any $i \in I_u(x)$, we consider the following four cases:

Case (1): $\eta_{i,j^*}(x, \tau^*) > 0$. In this case, $\lambda_{i,j^*}(x, \tau^*) = \frac{\omega_{i,j^*}(x, \tau^*)}{\eta_{i,j^*}(x, \tau^*)}$. Therefore, by (38) we have

$$\begin{aligned} & \eta_{i,j^*}(x, \tau^*) (\lambda^+(x) + \Delta_\lambda) \\ & \geq \underbrace{\eta_{i,j^*}(x, \tau^*) \lambda_{i,j^*}(x, \tau^*)}_{= \omega_{i,j^*}(x, \tau^*)} + \underbrace{\eta_{i,j^*}(x, \tau^*) \Delta_\lambda}_{> 0} \\ & > \omega_{i,j^*}(x, \tau^*), \end{aligned}$$

which shows the infeasibility of $\lambda^+(x) + \Delta_\lambda$ regarding the j^* -th component of the constraint of (27).

Case (2): $\eta_{i,j^*}(x, \tau^*) = 0$ and $\omega_{i,j^*}(x, \tau^*) \geq 0$. In this case, it follows from (29) that $\lambda^+(x) = \lambda_{i,j^*}(x, \tau^*) = 1$, which contradicts (38). Therefore, this case cannot occur.

Case (3): $\eta_{i,j^*}(x, \tau^*) = 0$ and $\omega_{i,j^*}(x, \tau^*) < 0$. It is straightforward to get that $\eta_{i,j^*}(x, \tau^*) (\lambda^+(x) + \Delta_\lambda) = 0 > \omega_{i,j^*}(x, \tau^*)$. Similar to case (1), it can be proved that $\lambda^+(x) + \Delta_\lambda$ is infeasible.

Case (4): $\eta_{i,j^*}(x, \tau^*) < 0$. Since $\lambda_{i,j^*}(x, \tau^*)$ can take either 0 or 1 in this case and recalling that $\lambda_{i,j^*}(x, \tau^*) < 1$, it must hold that $\lambda_{i,j^*}(x, \tau^*) = 0$ and that $\omega_{i,j^*}(x, \tau^*) - \eta_{i,j^*}(x, \tau^*) \lambda_{i,j''}(x, \tau'') < 0$, where $\lambda_{i,j''}(x, \tau'') = \min_{\tau'' \in [0, T], j'' \in \mathbb{N}_{\dim(\eta_i)}^+, \lambda_{i,j''}(x, \tau'') \in (0, 1)} \lambda_{i,j''}(x, \tau'')$. As a consequence, if $\lambda^+(x) + \Delta_\lambda \leq \lambda_{i,j''}(x, \tau'')$, we have

$$\begin{aligned} \eta_{i,j^*}(x, \tau^*) (\lambda^+(x) + \Delta_\lambda) & \geq \eta_{i,j^*}(x, \tau^*) \lambda_{i,j''}(x, \tau'') \\ & > \omega_{i,j^*}(x, \tau^*). \end{aligned} \quad (39)$$

If $\lambda^+(x) + \Delta_\lambda > \lambda_{i,j''}(x, \tau'')$, consider the j'' -th component of the constraint of (27). In particular, since $\lambda_{i,j''}(x, \tau'') \in (0, 1)$, by (29) we know that $\omega_{i,j''}(x, \tau'') > 0$, $\eta_{i,j''}(x, \tau'') > 0$, and $\lambda_{i,j''}(x, \tau'') = \frac{\omega_{i,j''}(x, \tau'')}{\eta_{i,j''}(x, \tau'')}$. Then we have

$$\begin{aligned} \eta_{i,j''}(x, \tau'') (\lambda^+(x) + \Delta_\lambda) & > \eta_{i,j''}(x, \tau'') \lambda_{i,j''}(x, \tau'') \\ & > \omega_{i,j''}(x, \tau''). \end{aligned} \quad (40)$$

Combining (39) and (40), we observe that either the j^* -th row or the j'' -th row of the constraint of (27) is violated for $\lambda^+(x) + \Delta_\lambda$ in Case (4).

Integrating the discussions in the four cases above and noticing the arbitrariness of i , we can conclude that $\lambda^+(x) + \Delta_\lambda$ is infeasible for problem (27).

- [1] A. Alan, A. J. Taylor, C. R. He, A. D. Ames, and G. Orosz, "Control barrier functions and input-to-state safety with application to automated vehicles," *IEEE Transactions on Control Systems Technology*, vol. 31, no. 6, pp. 2744–2759, 2023.
- [2] A. M. Jarrett, D. Faghihi, D. A. Hormuth, E. A. Lima, J. Virostko, G. Biros, D. Patt, and T. E. Yankelev, "Optimal control theory for personalized therapeutic regimens in oncology: Background, history, challenges, and opportunities," *Journal of Clinical Medicine*, vol. 9, no. 5, p. 1314, 2020.
- [3] F. Borrelli, A. Bemporad, and M. Morari, *Predictive Control for Linear and Hybrid Systems*. Cambridge University Press, 2017.
- [4] A. D. Ames, X. Xu, J. W. Grizzle, and P. Tabuada, "Control barrier function based quadratic programs for safety critical systems," *IEEE Transactions on Automatic Control*, vol. 62, no. 8, pp. 3861–3876, 2016.
- [5] S. Bansal, M. Chen, S. Herbert, and C. J. Tomlin, "Hamilton-Jacobi reachability: A brief overview and recent advances," in *2017 IEEE 56th Conference on Decision and Control (CDC)*, 2017, pp. 2242–2253.

[6] K. He, S. Shi, T. van den Boom, and B. De Schutter, "Approximate dynamic programming for constrained piecewise affine systems with stability and safety guarantees," *IEEE Transactions on Systems, Man, and Cybernetics: Systems*, vol. 55, no. 3, pp. 1722–1734, 2024.

[7] K. P. Wabersich and M. N. Zeilinger, "Predictive control barrier functions: Enhanced safety mechanisms for learning-based control," *IEEE Transactions on Automatic Control*, vol. 68, no. 5, pp. 2638–2651, 2022.

[8] —, "A predictive safety filter for learning-based control of constrained nonlinear dynamical systems," *Automatica*, vol. 129, p. 109597, 2021.

[9] T. Gurriet, M. Mote, A. Singletary, P. Nilsson, E. Feron, and A. D. Ames, "A scalable safety critical control framework for nonlinear systems," *IEEE Access*, vol. 8, pp. 187249–187275, 2020.

[10] Y. Chen, M. Jankovic, M. Santillo, and A. D. Ames, "Backup control barrier functions: Formulation and comparative study," in *2021 60th IEEE Conference on Decision and Control (CDC)*, 2021, pp. 6835–6841.

[11] D. E. Van Wijk, S. Coogan, T. G. Molnar, M. Majji, and K. L. Hobbs, "Disturbance-robust backup control barrier functions: Safety under uncertain dynamics," *IEEE Control Systems Letters*, vol. 8, pp. 2817–2822, 2024.

[12] J. Breedon and D. Panagou, "Predictive control barrier functions for online safety critical control," in *2022 IEEE 61st Conference on Decision and Control (CDC)*, 2022, pp. 924–931.

[13] A. Bemporad and M. Morari, "Control of systems integrating logic, dynamics, and constraints," *Automatica*, vol. 35, no. 3, pp. 407–427, 1999.

[14] A. Bemporad, F. Borrelli, and M. Morari, "Piecewise linear optimal controllers for hybrid systems," in *2000 American Control Conference*, vol. 2, 2000, pp. 1190–1194.

[15] T. Poggi, S. Trimboli, A. Bemporad, and M. Storace, "Explicit hybrid model predictive control: discontinuous piecewise-affine approximation and FPGA implementation," *IFAC Proceedings Volumes*, vol. 44, no. 1, pp. 1350–1355, 2011.

[16] S. Sadraddini and R. Tedrake, "Sampling-based polytopic trees for approximate optimal control of piecewise affine systems," in *2019 International Conference on Robotics and Automation (ICRA)*, 2019, pp. 7690–7696.

[17] P. Grieder, M. Kvasnica, M. Baotić, and M. Morari, "Stabilizing low complexity feedback control of constrained piecewise affine systems," *Automatica*, vol. 41, no. 10, pp. 1683–1694, 2005.

[18] C. F. O. da Silva, A. Dabiri, and B. De Schutter, "Integrating reinforcement learning and model predictive control with applications to microgrids," *arXiv preprint arXiv:2409.11267*, 2024.

[19] S. Mallick, A. Dabiri, and B. De Schutter, "Learning-based model predictive control for piecewise affine systems with feasibility guarantees," *arXiv preprint arXiv:2412.00490*, 2024.

[20] L. Russo, S. H. Nair, L. Glielmo, and F. Borrelli, "Learning for online mixed-integer model predictive control with parametric optimality certificates," *IEEE Control Systems Letters*, vol. 7, pp. 2215–2220, 2023.

[21] A. Didier, R. C. Jacobs, J. Sieber, K. P. Wabersich, and M. N. Zeilinger, "Approximate predictive control barrier functions using neural networks: A computationally cheap and permissive safety filter," in *2023 European Control Conference (ECC)*, 2023, pp. 1–7.

[22] K. He, S. Shi, T. van den Boom, and B. De Schutter, "State-action control barrier functions: Imposing safety on learning-based control with low online computational costs," *arXiv preprint arXiv:2312.11255*, 2023.

[23] K. He, S. Shi, T. v. d. Boom, and B. De Schutter, "From learning to safety: A direct data-driven framework for constrained control," *arXiv preprint arXiv:2505.15515*, 2025.

[24] T. G. Molnar and A. D. Ames, "Safety-critical control with bounded inputs via reduced order models," in *2023 American Control Conference (ACC)*, 2023, pp. 1414–1421.

[25] P. Glotfelter, J. Cortés, and M. Egerstedt, "Nonsmooth barrier functions with applications to multi-robot systems," *IEEE Control Systems Letters*, vol. 1, no. 2, pp. 310–315, 2017.

[26] A. Thirugnanam, J. Zeng, and K. Sreenath, "Nonsmooth control barrier functions for obstacle avoidance between convex regions," *arXiv preprint arXiv:2306.13259*, 2023.

[27] P. Ong, B. Capelli, L. Sabattini, and J. Cortés, "Nonsmooth control barrier function design of continuous constraints for network connectivity maintenance," *Automatica*, vol. 156, p. 111209, 2023.

[28] C. J. Cortes, M. Thitsa, and S. Coogan, "Discontinuous barrier functions for piecewise continuous dynamics," in *2024 American Control Conference (ACC)*, 2024, pp. 3987–3992.

[29] M. H. Cohen, P. Ong, G. Bahati, and A. D. Ames, "Characterizing smooth safety filters via the implicit function theorem," *IEEE Control Systems Letters*, vol. 7, pp. 3890–3895, 2023.

[30] A. D. Ames, S. Coogan, M. Egerstedt, G. Notomista, K. Sreenath, and P. Tabuada, "Control barrier functions: Theory and applications," in *2019 European Control Conference (ECC)*, 2019, pp. 3420–3431.

[31] K. P. Wabersich, A. J. Taylor, J. J. Choi, K. Sreenath, C. J. Tomlin, A. D. Ames, and M. N. Zeilinger, "Data-driven safety filters: Hamilton-Jacobi reachability, control barrier functions, and predictive methods for uncertain systems," *IEEE Control Systems Magazine*, vol. 43, no. 5, pp. 137–177, 2023.

[32] L. Wang, D. Han, and M. Egerstedt, "Permissive barrier certificates for safe stabilization using sum-of-squares," in *2018 American Control Conference (ACC)*, 2018, pp. 585–590.

[33] H. K. Khalil, *Nonlinear Systems*, 3rd ed. Prentice Hall, 2002.

[34] P. Mestres, A. Allibhou, and J. Cortés, "Regularity properties of optimization-based controllers," *European Journal of Control*, vol. 81, p. 101098, 2025.

[35] F. Clarke, "On the inverse function theorem," *Pacific Journal of Mathematics*, vol. 64, no. 1, pp. 97–102, 1976.

[36] B. S. Mordukhovich and N. M. N. and, "Geometric approach to convex subdifferential calculus," *Optimization*, vol. 66, no. 6, pp. 839–873, 2017.

[37] M. Lazar, W. Heemels, S. Weiland, and A. Bemporad, "Stabilizing model predictive control of hybrid systems," *IEEE Transactions on Automatic Control*, vol. 51, no. 11, pp. 1813–1818, 2006.

[38] F. H. Clarke, *Optimization and Nonsmooth Analysis*. SIAM, 1990.

[39] R. J. Aumann, "Integrals of set-valued functions," *Journal of Mathematical Analysis and Applications*, vol. 12, no. 1, pp. 1–12, 1965.

[40] H. P. Dicell, Jr, "An application of the Cayley-Hamilton theorem to generalized matrix inversion," *SIAM Review*, vol. 7, no. 4, pp. 526–528, 1965.

[41] D. Corona and B. De Schutter, "Adaptive cruise control for a SMART car: A comparison benchmark for MPC-PWA control methods," *IEEE Transactions on Control Systems Technology*, vol. 16, no. 2, pp. 365–372, 2008.

[42] J. F. Bonnans and A. Shapiro, *Perturbation Analysis of Optimization Problems*. Springer Science & Business Media, 2013.

[43] A. Ben-Tal and A. Nemirovski, "Robust convex optimization," *Mathematics of Operations Research*, vol. 23, no. 4, pp. 769–805, 1998.

[44] A. Richards and J. How, "Mixed-integer programming for control," in *2005 American Control Conference*, 2005, pp. 2676–2683.

[45] J. Tordesillas, J. P. How, and M. Hutter, "RAYEN: Imposition of hard convex constraints on neural networks," *arXiv preprint arXiv:2307.08336*, 2023.

[46] K. He, S. Shi, T. van den Boom, and B. De Schutter, "Efficient and safe learning-based control of piecewise affine systems using optimization-free safety filters," in *2024 IEEE 63rd Conference on Decision and Control (CDC)*, 2024, pp. 5046–5053.

[47] F. H. Clarke, "Generalized gradients and applications," *Transactions of the American Mathematical Society*, vol. 205, pp. 247–262, 1975.